

Spectral networks and Fenchel-Nielsen coordinates

Lotte Hollands¹ and Andrew Neitzke²

¹Mathematical Institute, University of Oxford

²Department of Mathematics, University of Texas at Austin

Abstract

We explain that spectral networks are a unifying framework that incorporates both shear (Fock-Goncharov) and length-twist (Fenchel-Nielsen) coordinate systems on moduli spaces of flat $SL(2, \mathbb{C})$ connections, in the following sense. Given a spectral network \mathcal{W} on a punctured Riemann surface C , we explain the process of “abelianization” which relates flat $SL(2)$ -connections (with an additional structure called “ \mathcal{W} -framing”) to flat \mathbb{C}^\times -connections on a covering $\Sigma \rightarrow C$. For any \mathcal{W} , abelianization gives a construction of a local Darboux coordinate system on the moduli space of \mathcal{W} -framed flat connections. There are two special types of spectral network, combinatorially dual to ideal triangulations and pants decompositions; these two types of network lead to Fock-Goncharov and Fenchel-Nielsen coordinates respectively.

Contents

1	Introduction	2
2	Spectral networks	6
2.1	Spectral networks	6
2.2	Fock-Goncharov networks	8
2.3	Fenchel-Nielsen networks	10
2.4	Contracted Fenchel-Nielsen network	12
2.5	Mixed spectral networks	13
3	WKB spectral networks	13
3.1	Foliations	15
3.2	Strebel differentials	16
3.3	A counterexample	17
4	Abelianization	18
4.1	What is abelianization?	18
4.2	Properties of abelianization	19
4.3	Equivalence of abelianizations	20

4.4	Spectral coordinates	20
4.5	Fock-Goncharov spectral networks	21
4.6	Fenchel-Nielsen spectral networks	26
4.7	Trivialization at boundary components	29
4.8	Mixed spectral networks	30
5	Nonabelianization	30
5.1	Almost-flat equivariant abelian representations	31
5.2	Nonabelianization map	33
6	Examples	35
6.1	Fock-Goncharov networks	35
6.1.1	Four-punctured sphere	35
6.1.2	Once-punctured torus	41
6.2	Fenchel-Nielsen examples	43
6.2.1	Pair of pants: molecule I	43
6.2.2	Pair of pants: molecule II	47
6.2.3	Four-holed sphere	48
6.2.4	Genus two surface	51
6.3	Mixed networks	51
7	Some consequences	52
7.1	Asymptotics	52
7.2	Line defects	53

1 Introduction

In the recent paper [1] a process called *nonabelianization* is described. Nonabelianization (along with its inverse, abelianization) is a way of studying flat connections in rank K vector bundles over a surface C by relating them to far simpler objects, namely connections in rank 1 bundles over K -fold branched covers of C . The main new result of this paper is that abelianization gives a new way of thinking about a rather classical object, namely the *Fenchel-Nielsen coordinate system* on the moduli space of $PSL(2)$ connections over C .

Before describing the result let us briefly review what nonabelianization is. Suppose given a flat connection ∇^{ab} in a rank 1 bundle over a branched cover Σ of C . A naive way of relating ∇^{ab} to a rank K connection over C would be just to take the pushforward. This indeed gives a connection ∇ in a rank K bundle over C , or more precisely over the complement of the branch locus in C . However, this connection does *not* extend smoothly over the branch locus. The reason is simple: when one goes around a branch point of the covering $\Sigma \rightarrow C$, the sheets of Σ are permuted, and this permutation shows up as a nontrivial monodromy for the pushforward connection ∇ . Thus ∇ so defined cannot be extended to a flat connection on the whole of C .

The nonabelianization operation is a recipe for “fixing up” this monodromy problem, by cutting the surface C into pieces, then regluing the connection ∇ with some nontrivial automorphisms along the gluing lines. The collective effect of this cutting-and-gluing is to cancel the unwanted monodromy while not creating any monodromy anywhere else.

The cutting-and-gluing is done along a collection of paths on the surface which is called a *spectral network*. To be precise, a spectral network is a collection of paths on a surface C , carrying some extra labels and obeying some conditions; see §2.1 below for a definition sufficient for our purposes in this paper. (Spectral networks were described in [1], where it was shown that they are a fundamental ingredient in the story of BPS states and wall-crossing for $\mathcal{N} = 2$ supersymmetric quantum field theories of “class S ” [2, 3]. For subsequent work on spectral networks in $\mathcal{N} = 2$ theories see [4, 5, 6, 7]. Essentially the same object has also been considered in the mathematical literature on Stokes phenomena, e.g. [8].)

Once we have a particular spectral network \mathcal{W} in hand, we can define the nonabelianization operation, as well as its inverse, abelianization. To emphasize that this operation depends on \mathcal{W} , let us call it \mathcal{W} -abelianization. It turns out that for many choices of the network \mathcal{W} there is an almost unique way of \mathcal{W} -abelianizing a given generic connection ∇ . (“Almost” here means that there may be some discrete choices to be made, which in this paper we encapsulate in a notion of \mathcal{W} -framed connection.) Once we have made these choices, we get a unique \mathcal{W} -abelianization for a \mathcal{W} -framed connection ∇ .

In particular, given a \mathcal{W} -framed connection ∇ and some $\gamma \in H_1(\Sigma, \mathbb{Z})$ one can ask: what is the holonomy around γ of the connection ∇^{ab} which \mathcal{W} -abelianizes ∇ ? Let $\mathcal{X}_\gamma(\nabla) \in \mathbb{C}^\times$ denote the answer to this question. The collection of numbers $\mathcal{X}_\gamma(\nabla)$ in many cases suffice to determine the connection ∇ . We thus get a local coordinate system on the moduli space of \mathcal{W} -framed flat connections ∇ ; call this the *spectral coordinate system* associated to the network \mathcal{W} .

In this paper we take a close look at the spectral coordinate systems in the case $K = 2$. For the reader’s convenience, we first consider a class of spectral networks which had actually been considered earlier, in [4]. For these networks it was shown in [4] (for all $K \geq 2$) that the spectral coordinates are the same as some coordinates introduced earlier by Fock and Goncharov [9]. With this in mind we call these networks “Fock-Goncharov networks.” We give a self-contained re-derivation in the special case $K = 2$ of the fact that Fock-Goncharov networks induce Fock-Goncharov coordinates. We also clarify a few points which might be obscure in [4]; in particular we are more careful about how the story depends on whether we consider connections for the group $GL(2)$, $SL(2)$ or $PSL(2)$.

We then move on to consider a new class of spectral networks, which we call Fenchel-Nielsen networks. As we explain, the corresponding spectral coordinates are a complexified version of Fenchel-Nielsen (length-twist) coordinates.¹ Thus, *abelianization via spectral networks is a unifying framework which incorporates both Fock-Goncharov and Fenchel-Nielsen coordinate systems*.

¹Length-twist coordinates were originally defined by Fenchel and Nielsen, in a manuscript recently published as [10]. See also [11, 12]. A complex version of Fenchel-Nielsen coordinates was found in [13, 14, 15].

Spectral networks and quadratic differentials

One suggestive way of understanding the above result comes from the connection between spectral networks and quadratic differentials. Every meromorphic quadratic differential φ_2 on C induces a corresponding spectral network $\mathcal{W}(\varphi_2)$, the “critical graph” of φ_2 . For generic φ_2 the resulting $\mathcal{W}(\varphi_2)$ is a Fock-Goncharov network; this is the basic reason why the previous work [3] focused on Fock-Goncharov networks and the associated Fock-Goncharov coordinate systems.

This motivates the question: what about *non-generic* φ_2 ? If φ_2 is not generic then we obtain more general kinds of networks, called *mixed* in this paper. In particular, if φ_2 is in a certain sense maximally non-generic, i.e. if it is a Strebel differential, the corresponding network $\mathcal{W}(\varphi_2)$ is a Fenchel-Nielsen network.

Motivations from physics

Another motivation for being interested in Fenchel-Nielsen networks comes from the link between spectral networks and $\mathcal{N} = 2$ supersymmetric field theories. Recall that given a punctured Riemann surface C there is a corresponding $\mathcal{N} = 2$ theory $S[A_1, C]$ as discussed in [16, 3, 2]. The quadratic differentials φ_2 just discussed correspond to points of the Coulomb branch of this theory.

In some approaches to understanding the AGT correspondence [17], complexified Fenchel-Nielsen coordinates on the moduli of $SL(2)$ connections play an important role. For example, in [15] a semiclassical limit of the Nekrasov partition function of the theory $S[A_1, C]$ gets identified with the generating function, in complexified Fenchel-Nielsen coordinates, of the variety of opers inside the moduli space of flat $SL(2)$ -connections on C . Fenchel-Nielsen coordinates are also important in the interpretation of the AGT correspondence given in [18].

The result of this paper gives a new way of understanding the role of Fenchel-Nielsen coordinates in the theories $S[A_1, C]$, and thus may shed further light on these approaches. We limit ourselves here to a few optimistic comments, as follows.

- First, in this paper the complexified Fenchel-Nielsen coordinates get linked to a particular locus of the Coulomb branch, corresponding to the set of Strebel differentials. This locus is a “real” subspace inside the Coulomb branch: indeed, it is the locus where all of the vector multiplet scalars a^I are real, with respect to a particular choice of electromagnetic frame corresponding to the pants decomposition. It is interesting that this real subspace has played a distinguished role in applications to $\mathcal{N} = 2$ theory in the past. For example, in the computation of the S^4 partition function via localization [19], one naturally considers integrals not over the whole Coulomb branch but rather over this real subspace. Also, it appears that the spectrum of framed BPS states at this real subspace is especially simple: as we describe in §7.2 below, at this locus the UV line defects corresponding to Wilson loops carry just two framed BPS states, exactly matching the naive classical expectation.
- One would like to extend the approaches of [15, 18] to other Lie algebras, e.g. to the case A_{K-1} . The question then arises: *what is the higher rank analogue of Fenchel-Nielsen*

coordinates?

In this paper we find that Fenchel-Nielsen coordinates correspond to the spectral networks which appear at a real locus of the Coulomb branch for $K = 2$. This suggests that one might be able to find higher rank Fenchel-Nielsen coordinates in a similar way, by studying spectral networks appearing at a real locus of the Coulomb branch for $K > 2$.

- The constructions of [18] make use of a correspondence between Fenchel-Nielsen length coordinates ℓ^I and local coordinate functions a^I on the Coulomb branch of the $\mathcal{N} = 2$ theory, i.e. on the Hitchin base. The invariant meaning of this correspondence is a bit mysterious at first glance. After all, ℓ^I and a^I are not the same. Both of them can be viewed as functions on the moduli space of flat connections, but they are holomorphic in *different* complex structures on that space — the ℓ^I are holomorphic in the usual complex structure, while the a^I are holomorphic after rotating to the Higgs bundle complex structure. The correct relation between the two is an *asymptotic* one, of the schematic form $\ell^I \sim \exp(a^I/\zeta)$ as $\zeta \rightarrow 0$, obtained by applying the WKB approximation to certain 1-parameter families of flat connections. Of course, this relation is noted in [18] too. What we add here is just the observation that this asymptotic relation — and an understanding of its precise range of validity — arises quite naturally from the point of view of the Fenchel-Nielsen spectral networks; see §7.1 below.

Organization

We define the notion of a spectral network in §2 and introduce the particular classes that we will consider in this paper. This includes the Fock-Goncharov and Fenchel-Nielsen type spectral networks mentioned above. In §3 we recall the relation between spectral networks and meromorphic quadratic differentials, i.e. points on the Coulomb branch. In §4 we explain how a \mathcal{W} -framed $SL(2)$ connection ∇ can be abelianized to obtain an almost-flat equivariant abelian connection ∇^{ab} over a branched double cover $\Sigma \rightarrow C$, and how this construction yields the spectral coordinates \mathcal{X}_γ on the moduli space of flat \mathcal{W} -framed flat $SL(2)$ -connections. Furthermore, we argue that the spectral coordinates associated to Fock-Goncharov and Fenchel-Nielsen networks are complexified shear (Fock-Goncharov) and length-twist (Fenchel-Nielsen) coordinates respectively.

In §5 we discuss the inverse construction, \mathcal{W} -nonabelianization, where we begin with the spectral coordinates (or equivalently with the abelian connection ∇^{ab}) and build the corresponding \mathcal{W} -framed flat $SL(2)$ -connection ∇ . \mathcal{W} -nonabelianization was also considered in [1], but here we give a more explicit version, which directly gives concrete matrices representing the parallel transport of ∇^{ab} . In particular, in §6 we re-verify by explicit computation in several examples that the shear and length-twist coordinates occur as spectral coordinates for Fock-Goncharov and Fenchel-Nielsen networks respectively.

Finally, in §7 we discuss a few potential applications of our main new result, that Fenchel-Nielsen coordinates occur as spectral coordinates. One such application concerns the asymptotic behavior of Fenchel-Nielsen coordinates along certain one-parameter families of connections: interpreting these coordinates as spectral coordinates means that

these asymptotics should be controlled by period integrals on Σ in a precise way (essentially by applying the WKB approximation). A second application concerns the spectrum of framed BPS states attached to Wilson line defects in the theory $S[A_1, C]$.

Acknowledgements

We thank Anna Wienhard for a very helpful discussion. The research of LH has been supported by an NWO Rubicon fellowship and is now supported by a Royal Society Dorothy Hodgkin fellowship. LH also thanks the Junior Program of the Hausdorff Research Institute for hospitality. The research of AN is supported by NSF grant 1151693. This work was furthermore supported in part by the National Science Foundation under Grant No. PHYS-1066293 and we thank the hospitality of the Aspen Center for Physics.

2 Spectral networks

In this section we start with the definition of spectral network, and then introduce the particular classes of spectral networks we will consider in this paper.

We first describe the class of “Fock-Goncharov networks.” Such networks are associated to ideal triangulations of the surface C . They played the starring role in [3]. Second, we introduce a new class of spectral networks which we call “Fenchel-Nielsen networks.” These networks are associated to pants decompositions of the surface C rather than triangulations. They have not been considered explicitly before. Third, we briefly consider two more general kinds of network: one obtained by collapsing some double walls in a Fenchel-Nielsen network, which we call “contracted Fenchel-Nielsen”, and another which is part Fock-Goncharov and part Fenchel-Nielsen, which we call “mixed”.

2.1 Spectral networks

Before introducing the notion of spectral network, let us fix some notations and conventions:

- C will always denote a real surface of negative Euler characteristic. C may have punctures and/or boundary components.²
- Σ will denote a branched double cover of C , which restricts to a trivial cover in a neighborhood of each puncture or boundary component.

We often find it convenient to choose a set of branch cuts on C and trivialize the cover Σ , labeling its sheets as “sheet 1” and “sheet 2” on the complement of the branch cuts.

A *spectral network* \mathcal{W} subordinate to Σ is then a collection of oriented paths w on C , which we call *walls*, with the following properties and structure:

- Each wall w begins at a branch point of $\Sigma \rightarrow C$, and ends either at a puncture or at a branch point. A wall ends at a branch point if and only if it coincides with an

²In figures we sometimes draw a marked point on each boundary component. These marked points become relevant later, when we discuss \mathcal{W} -framed connections on C that are trivialized at the boundary.

oppositely oriented wall. We say that the locus where two walls coincide is a “double wall”.

- Walls never intersect one another or themselves, except that it is possible for two oppositely oriented walls to coincide, as we have just remarked.
- Each wall w carries an ordering of the 2 sheets of the covering Σ over w . If we have fixed a labeling of the sheets, this amounts to saying w locally carries either the label 12 or 21, and the label changes when w crosses a branch cut.

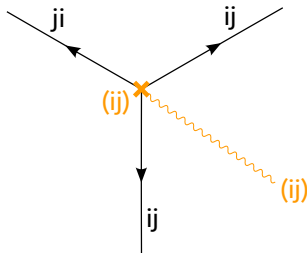


Figure 1: Local configuration of walls near a branch point.

- Exactly three walls w begin at each branch point, and consecutive walls carry opposite sheet orderings; see Figure 1.
- The two constituents in a double wall carry opposite sheet orderings: thus, if we have fixed a labeling of the sheets, then locally one is labeled 12 and the other 21.
- If there is at least one double wall, then the network comes with an additional discrete datum, the choice of a *resolution*, which is one of the two words “British” or “American”. We think of the resolution as telling us how the two constituents of each double wall are infinitesimally displaced from one another; see Figure 2 for the rules.
- The spectral network carries a *decoration*, to be defined below.

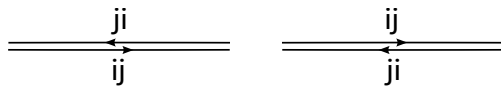


Figure 2: Left: a double wall with American resolution. Right: a double wall with British resolution.

In this paper we restrict ourselves to spectral networks with some extra topological properties. First, the covering Σ should have exactly $-2\chi(C)$ branch points, all of which are simple. Second, the closure of each connected component of $C \setminus \mathcal{W}$ must either have one of the topologies shown in Figure 3, or be obtained from one of those topologies by some identifications along the boundary. In particular, each puncture has at least one wall ending on it, whereas boundary components have no walls ending on them.

With this restriction we can now explain what a decoration is. First:

- A decoration of a puncture $z_i \in C$ is an ordering of the sheets of Σ over z_i . The labels of all walls which end on z_i must match the decoration at the puncture.

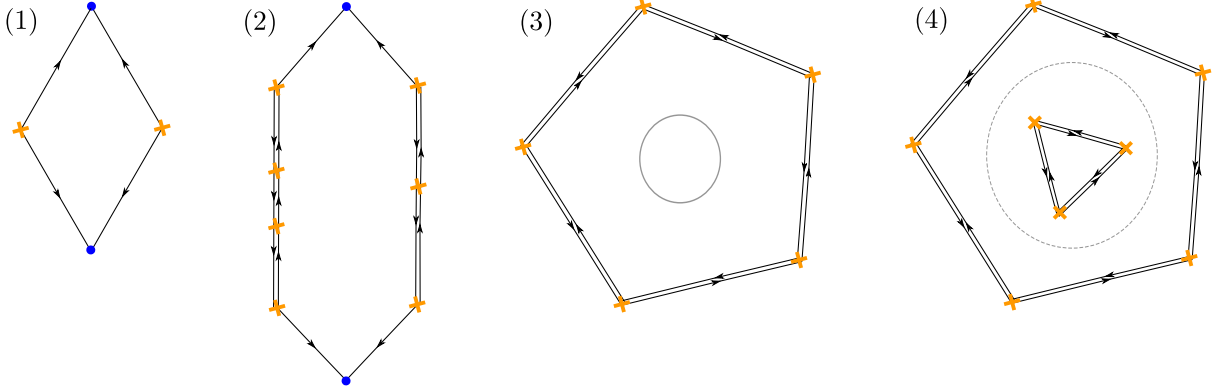


Figure 3: Possible topologies for the connected components of $C \setminus \mathcal{W}$: (1) Generic cell with two punctures and two branch points as vertices. (2) Degenerate cell which has two punctures and can have any number of branch points as vertices. Every pair of neighbouring branch points is connected by a double wall. (3) A tubular region bounded by a boundary component on one side and a double wall on the other. (4) A tubular region bounded by a double wall, with the same resolution, on either side.

- A decoration of a boundary component or interior annulus is an ordering of the sheets for each way of going around it. The label of any wall that runs parallel to the boundary component or annulus must match the decoration in that direction.

Then a decoration of \mathcal{W} means a collection of decorations, one for each puncture, boundary component or interior annulus of \mathcal{W} .

Let us emphasize that while the punctures, marked points and branch points are part of the definition of a spectral network, the branch cuts and the labeling of the sheets are not: they just come in handy when we want to draw figures and work out explicit examples.

2.2 Fock-Goncharov networks

Suppose that C has at least one puncture, but no boundary components. Fix an *ideal triangulation* \mathcal{T} of C , i.e. a triangulation for which the set of vertices is precisely the set of punctures on C .³

Now we can construct the Fock-Goncharov network corresponding to \mathcal{T} . First, mark one point b in each triangle of \mathcal{T} , and let $\Sigma \rightarrow C$ be the unique double cover which is branched exactly at these points. Next, for each branch point b , draw three oriented paths from b to the three vertices of the triangle in which b sits. These paths are the walls making up the spectral network. Examples are shown in Figures 4 and 5.

According to the definition of spectral network in §2.1 we must decorate each wall w with an ordering of the two sheets of the cover Σ over w , and we must also decorate each puncture with an ordering of the two sheets near the puncture (see Figure 4 for an

³We could allow \mathcal{T} to include some “degenerate” triangles, obtained e.g. by gluing together two vertices or two edges of an ordinary triangle; see [9, 3] for the precise class of triangulations one can allow.

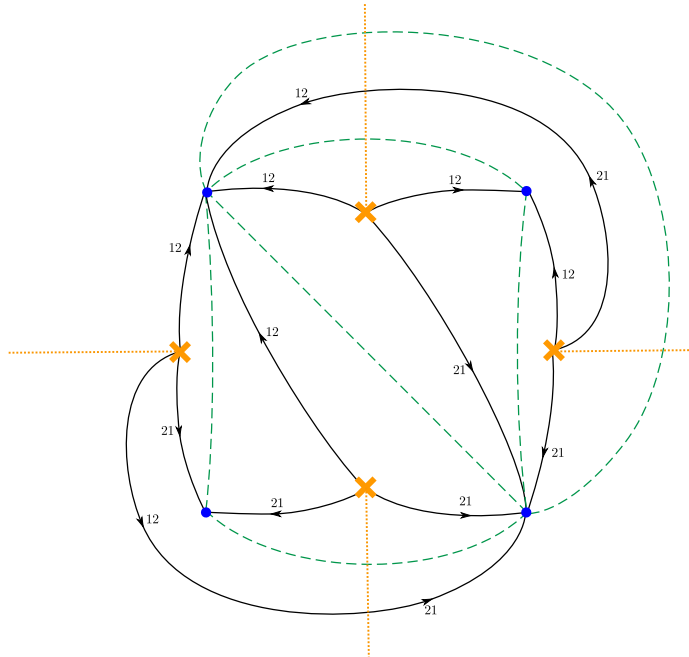


Figure 4: Example of a Fock-Goncharov network on the four-punctured sphere. Walls are drawn as oriented black lines. Orange crosses are branch points, dashed orange lines are branch cuts. The dual ideal triangulation is given by the dashed green lines.

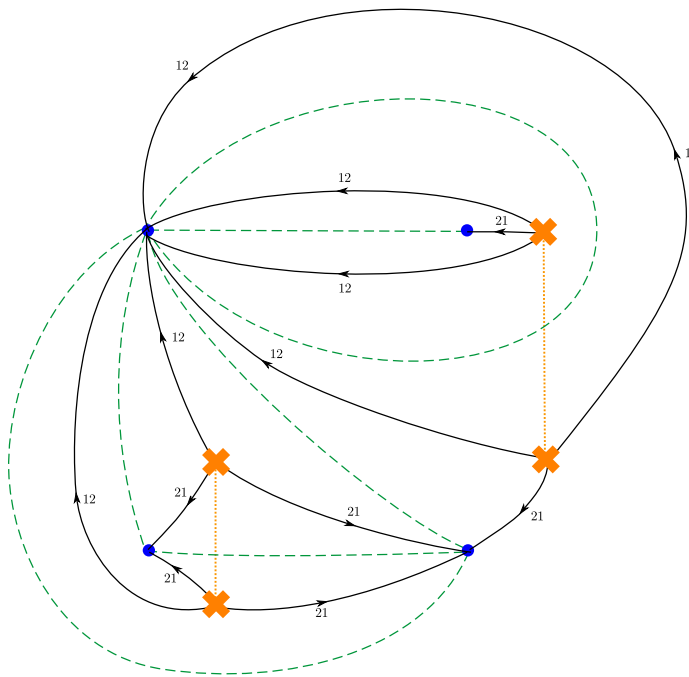


Figure 5: Example of a Fock-Goncharov network on the four-punctured sphere. The dual (degenerate) ideal triangulation is given by the dashed green lines.

example). These data are subject to some constraints: first, if a wall w ends on a puncture p the label on w and on p must be the same; second, two consecutive walls emerging from the same branch point must carry opposite labels (unless we cross a branch cut in moving from one to the next). Altogether these rules imply that once we choose the label on a single wall, the labels on all other walls in the spectral network are fixed.

2.3 Fenchel-Nielsen networks

Now consider a surface C with no punctures, but possibly with boundary components. Also suppose given a pants decomposition of C . We consider spectral networks whose restriction to each pair of pants is either *molecule I* (Figure 6) or *molecule II* (Figure 7).⁴ We call any such network a “Fenchel-Nielsen network”. As for any spectral network there are three outgoing walls at every branch point. For the Fenchel-Nielsen networks, however, every wall also *ends* at a branch point. All its walls are thus double walls.

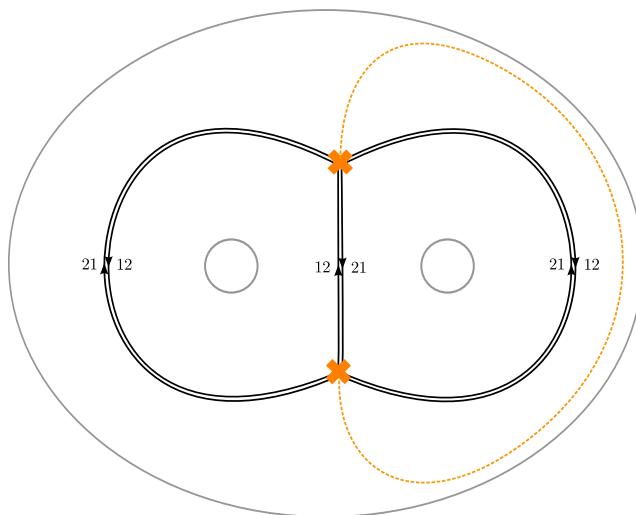


Figure 6: Molecule I: first example of a Fenchel-Nielsen spectral network on a pair of pants. The network carries the “British resolution”; to get the “American resolution” one would swap the orientation of every wall in the network.

The double walls of a Fenchel-Nielsen network are decorated according to the rules in §2.1 (see for example Figure 6 and Figure 7). All connected components A of $C \setminus \mathcal{W}$ have the topology of an annulus, and should thus also be decorated. As explained in §2.1, we choose a label for each way of going around A that matches the decoration of the nearest wall. When two boundary components are glued, their decorations must agree (an example is given in Figure 8). These rules fix the decoration of walls and connected components of any Fenchel-Nielsen network once we have chosen a label on a single wall.

⁴Molecule I and molecule II are *not* isotopic, since for any homotopy the two branch points have to pass through each other. This will become clear later, when we introduce spectral coordinates: the spectral coordinates for molecule I are not equal to those for molecule II.

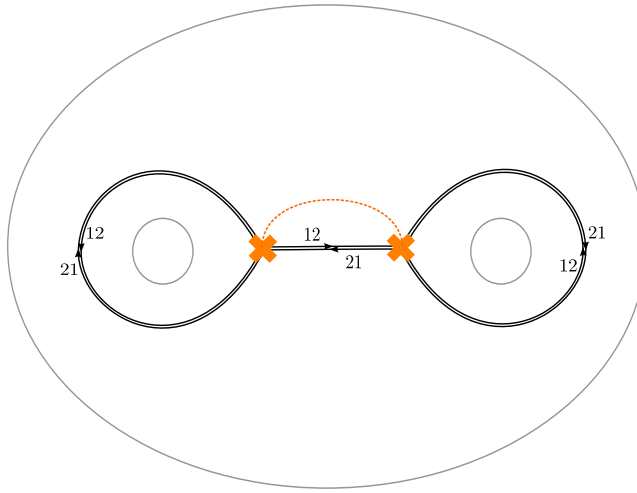


Figure 7: Molecule II: second example of a Fenchel-Nielsen spectral network on a pair of pants. The network carries the “British resolution”; to get the “American resolution” one would swap the two lanes on each street.

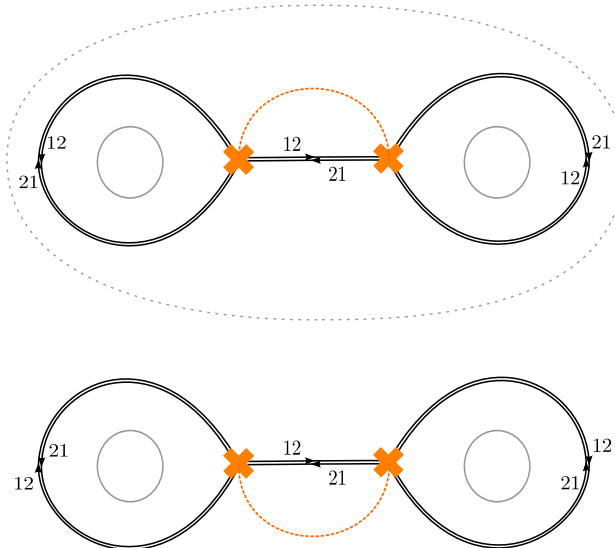


Figure 8: Example of a Fenchel-Nielsen spectral network on the four-holed sphere.

We remark that there is a sense in which a Fenchel-Nielsen network can be considered as a limit of Fock-Goncharov networks. See Figures 9 and 10. This limiting procedure has a particularly transparent meaning if we consider the spectral networks as coming from quadratic differentials on C . We explain this in §3.

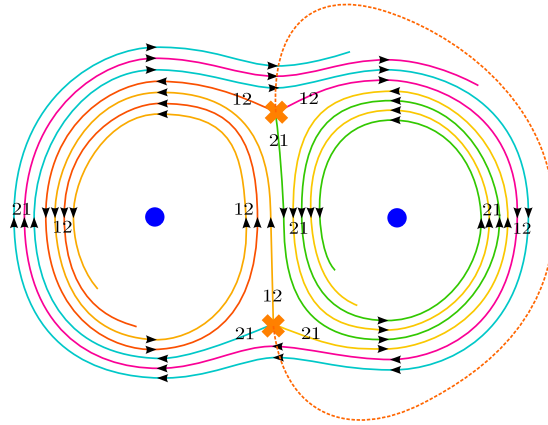


Figure 9: Example of a spectral network on the three-punctured sphere, all of whose walls wind a large number of times around the punctures and eventually end on them. In the limit of infinite windings this spectral network turns into the British resolution of molecule I.

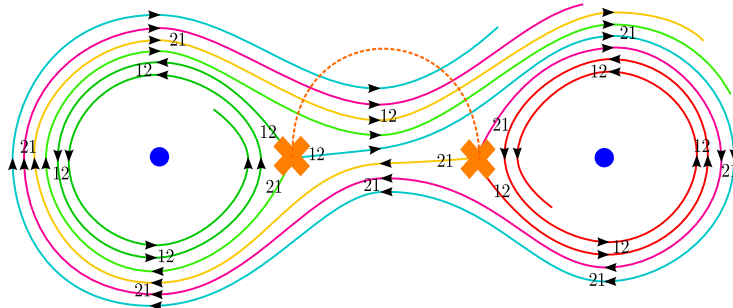


Figure 10: Example of a spectral network on the three-punctured sphere, all of whose walls wind a large number of times around the punctures and eventually end on them. In the limit of infinite windings this spectral network turns into the British resolution of molecule II.

2.4 Contracted Fenchel-Nielsen network

There is a larger class of spectral networks in which all walls are double walls. An example of a spectral network in this class that is not a Fenchel-Nielsen network is given in Figure 11. We refer to such a network as a *contracted* Fenchel-Nielsen network.

A contracted Fenchel-Nielsen network can be obtained by degeneration of a regular Fenchel-Nielsen network. This is illustrated in Figure 12. In the degeneration limit a

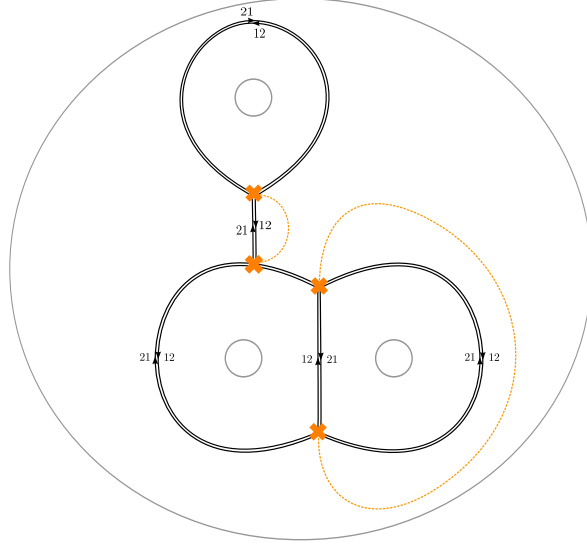


Figure 11: Example of contracted Fenchel-Nielsen network on the four-holed sphere.

single double wall in one component of the regular spectral network limits to a set of double walls in another component of the regular spectral network.

In fact, one may obtain a single contracted Fenchel-Nielsen network from several distinct ordinary Fenchel-Nielsen networks in this way. The distinct choices of regular networks that limit to the same contracted network are associated to different pants decompositions.

2.5 Mixed spectral networks

We call any other type of spectral network that contains both single and double walls a mixed spectral network. An example is given in Figure 13.

3 WKB spectral networks

In this section we review how many spectral networks can be generated by meromorphic quadratic differentials φ_2 on C . Networks which can be obtained in this way are known as *WKB spectral networks*. The class of WKB spectral networks overlaps with all classes of spectral networks that we have introduced previously.

The quadratic differential φ_2 is *not* directly relevant to abelianization of $SL(2)$ connections, and thus will play no role in the next few sections. However, the construction of WKB spectral networks might clarify our rather abstract definition of a spectral network, and will be relevant again in the applications in §7.

As we will describe, a generic quadratic differential φ_2 generates a Fock-Goncharov network, whereas a Fenchel-Nielsen type spectral network comes from a φ_2 that has real periods around each pants curve. Such a φ_2 is known as a *Strebel differential*.

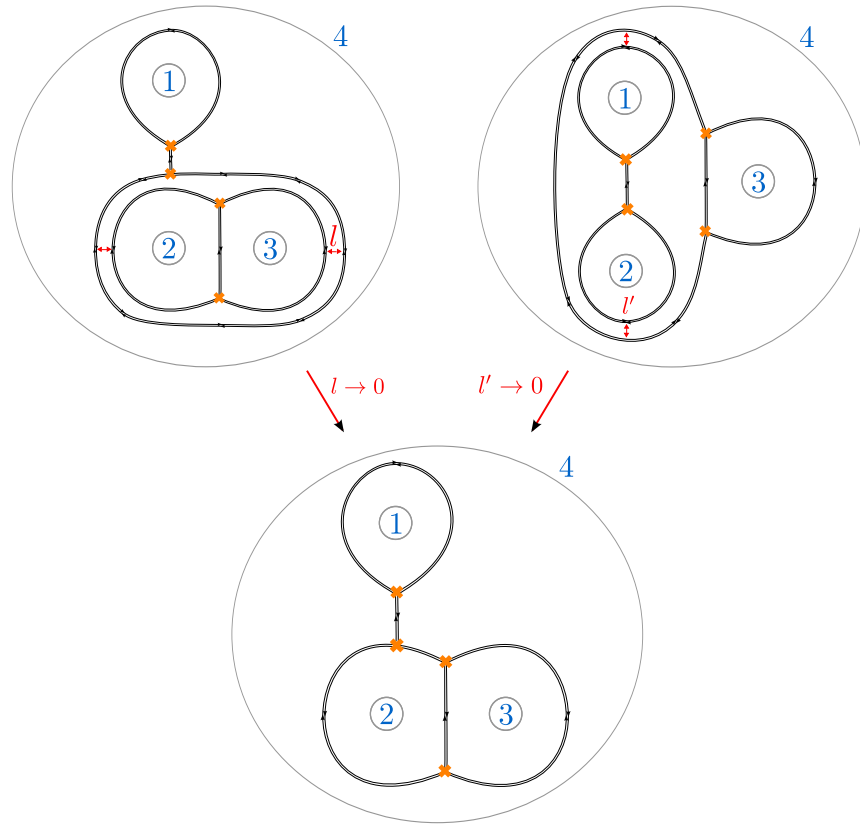


Figure 12: A contracted Fenchel-Nielsen network on the four-holed sphere, which can be obtained in a degeneration limit from two distinct (regular) Fenchel-Nielsen networks. These (regular) Fenchel-Nielsen networks are associated to two different choices of pants decomposition of the four-holed sphere.

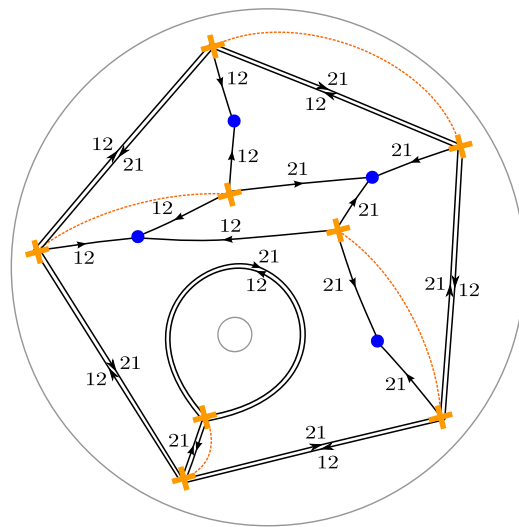


Figure 13: A mixed spectral network on a sphere with four punctures and two holes.

In the physical application to theories of class $S[A_1]$, quadratic differentials parameterize the Coulomb branch. Fock-Goncharov networks thus appear at generic points of the Coulomb branch, whereas Fenchel-Nielsen networks appear at a real locus.

3.1 Foliations

Let C be a punctured Riemann surface and let φ_2 be a meromorphic quadratic differential on \bar{C} , holomorphic on the complement of the punctures z_i . Locally such a differential is given by

$$\varphi_2 = u(z)(dz)^2. \quad (3.1)$$

We suppose that φ_2 has only simple zeroes on C , and second-order poles at the punctures z_i , with residue $-m_i^2$.

Fixing an angle ϑ , there is a singular foliation $\mathcal{F}(\varphi_2, \vartheta)$ on C , with angle ϑ , whose leaves are real curves $\gamma(t)$ along which

$$e^{-2i\vartheta} u(\gamma(t)) \left(\frac{d\gamma(t)}{dt} \right)^2 \geq 0. \quad (3.2)$$

(When $\vartheta = 0$ this is sometimes called the “horizontal foliation” attached to φ_2 .) The foliation $\mathcal{F}(\varphi_2, \vartheta)$ has singularities only at the zeroes and poles of φ_2 . Around a pole z_i the foliation depends on the value of $e^{-i\vartheta} m_i$, as illustrated in Figure 14. In the neighborhood

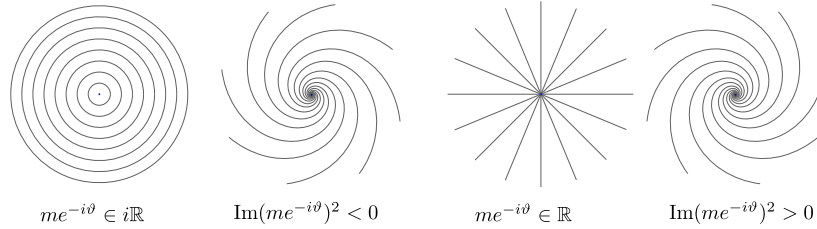


Figure 14: The behavior of the foliation $\mathcal{F}(\varphi_2, \vartheta)$ around a pole of φ_2 .

of a zero of φ_2 the foliation looks like Figure 15.

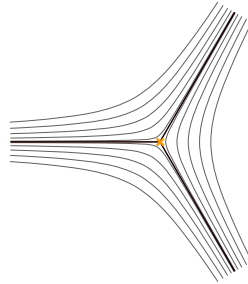


Figure 15: The behavior of the foliation $\mathcal{F}(\varphi_2, \vartheta)$ around a zero of φ_2 .

A leaf is called “critical” when the left-hand side of (3.2) vanishes at one end of the open interval. If we define the cover Σ by the equation

$$w^2 = u(z), \quad (3.3)$$

the zeroes of $u(z)$ are the branch points of the double covering. A leaf is thus critical if and only if it has one end on a branch point on C . The union of the critical leaves is known as the *critical graph* $CG(\varphi_2, \vartheta)$ of the foliation.

The critical graph $CG(\varphi_2, \vartheta)$ can be turned into a spectral network. Indeed, there are exactly three critical leaves emanating from each branch point, all critical leaves have at least one end on a zero of φ_2 , and the other endpoint can be either a zero or a singularity. A spectral network is obtained if we orient each non-compact critical leaf such that it originates from a branchpoint, if we replace each compact critical leaf by two coincident oppositely oriented walls, and if we choose a labeling of the resulting oriented walls according to the rules in §2.1. The spectral network so obtained is called a *WKB spectral network*.

For generic (φ_2, ϑ) all leaves of $\mathcal{F}(\varphi_2, \vartheta)$ end at singularities. If C is punctured, a generic critical graph $CG(\varphi_2, \vartheta)$ is dual to an ideal triangulation and thus determines a Fock-Goncharov network. An example is given in Figure 16.

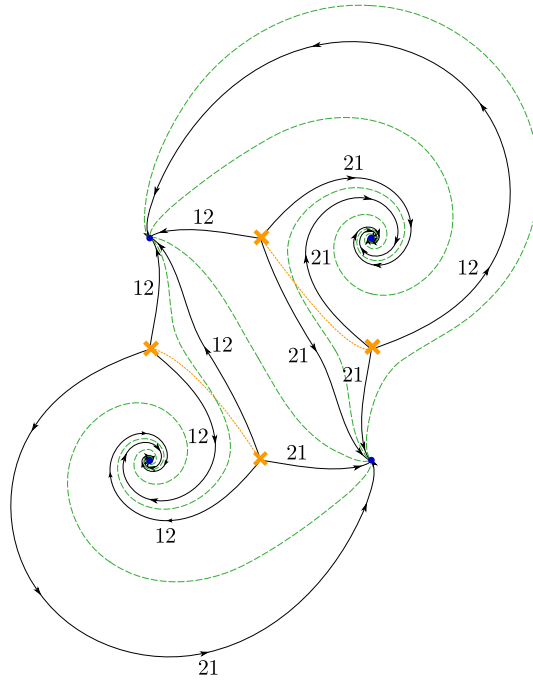


Figure 16: Example of a generic WKB spectral network on the four-punctured sphere. Here φ_2 is given by $u(z) = \frac{(z-1)(z+1)(z-i)(z+i)}{(z+(1-i))(z+(-1-i))(z+(1+i))(z+(-1+i))}$ and $\vartheta = \frac{2\pi}{3}$. The dashed green lines represent the corresponding ideal triangulation.

3.2 Strebel differentials

Suppose that the foliation does contain a family of compact leaves. This is for instance the case if we tune ϑ such that

$$\text{Im}(e^{-i\vartheta} m_i) = 0 \tag{3.4}$$

where m_i^2 is the coefficient of a quadratic pole in φ_2 . The resulting family of compact leaves is bounded by a polygon of compact critical leaves.

Any such foliation with a family of compact leaves turns into a generic one when ϑ is varied slightly. Moreover, if we vary ϑ from ϑ^- to ϑ^+ the foliation undergoes a topology change: clockwise spiraling leaves transform into anti-clockwise spiraling leaves, or vice-versa. This is illustrated in Figure 17.

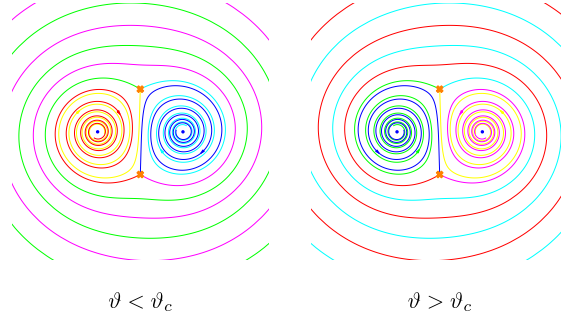


Figure 17: The foliation $\mathcal{F}(\varphi_2, \vartheta)$ near a critical phase ϑ_c where a family of compact leaves appears.

A quadratic differential φ_2 is called “Strebel” if its horizontal foliation $\mathcal{F}(\varphi_2, 0)$ has *only* compact leaves. This implies that each component of the complement of the critical graph is a union of cylinders swept out by homotopic leaves. Applying our rules to such a foliation we obtain a Fenchel-Nielsen spectral network (either regular or contracted).

Strebel’s theorem tells us that given a pants decomposition P of C and $3g - 3 + 2n$ positive real numbers $m_j \in \mathbb{R}_+$, there is a unique Strebel differential whose system of compact leaves is homotopic to the system of simple closed curves defining P , and such that m_j is the circumference of the polygon α_j of critical leaves that surround each puncture or tube,

$$m_j = \oint_{\alpha_j} \sqrt{u} dz, \quad (3.5)$$

where the branch of the square root is chosen so that $m_j > 0$.

As an example, the unique Strebel differential on the three-punctured sphere is defined by

$$\varphi_2 = -\frac{m_\infty^2 z^2 - (m_\infty^2 + m_0^2 - m_1^2)z + m_0^2}{4\pi^2 z^2(z-1)^2} (dz)^2. \quad (3.6)$$

It has double poles at the punctures $z_i = 0, 1, \infty$ with coefficients $-\frac{m_0^2}{4\pi^2}, -\frac{m_1^2}{4\pi^2}, -\frac{m_\infty^2}{4\pi^2} \in \mathbb{R}_-$, respectively. This differential generates the spectral network which we called “molecule I” when $m_\infty < m_0 + m_1$ and “molecule II” when $m_\infty > m_0 + m_1$.

3.3 A counterexample

We finish this section with the remark that not all spectral networks arise as WKB spectral networks. An illustrative example is given in Figure 18. If it were possible to

generate this spectral network by a quadratic differential, the lengths of the critical leaves would need to obey

$$\begin{aligned} m_1 + m_6 &= m_1 + m_2 + m_3 + m_4, \\ m_4 + m_5 &= m_2 + m_3 + m_5 + m_6. \end{aligned}$$

Clearly, this is impossible for positive real parameters m_1, \dots, m_6 .⁵

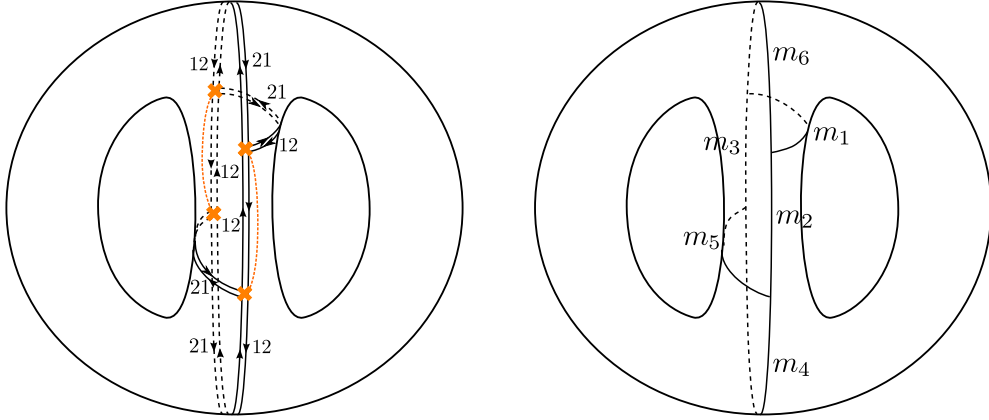


Figure 18: Left: example of a spectral network that cannot be generated by a quadratic differential. Right: critical leaves of the corresponding foliation.

4 Abelianization

What is a spectral network good for? Here is one answer: given a spectral network \mathcal{W} and a generic flat $SL(2, \mathbb{C})$ connection ∇ over C , we can construct a \mathcal{W} -abelianization of ∇ . This is the key to the construction of the “spectral coordinate” systems on the moduli of flat $SL(2, \mathbb{C})$ connections. In this section we explain this construction.

4.1 What is abelianization?

Let us first explain informally what we mean by \mathcal{W} -abelianization. A \mathcal{W} -abelianization is a way of putting ∇ in almost-abelian form. Namely, in each component of $C' = C \setminus \mathcal{W}$ we will find a gauge relative to which ∇ is valued in the diagonal subalgebra of $sl(2, \mathbb{C})$; call such a gauge “abelian.” Of course our abelian gauges on the components of C' usually are not the restriction of a single global abelian gauge on C (it would be impossible to globally diagonalize a generic ∇). However, we will get close to this ideal situation: the abelian gauges on two sides of a wall $w \subset \mathcal{W}$ will be related by a gauge transformation which is *unipotent*, either upper or lower triangular, according as the wall is labeled 12

⁵This example appears in [20], as an example of a measured foliation which cannot be generated by a quadratic differential. Although the measured foliation is equivalent to one that can be generated by a quadratic differential, this is not the case for the associated spectral network.

or 21. Similarly, the gauges on two sides of a branch cut for the covering $\Sigma \rightarrow C$ will be related by a permutation matrix.

If ∇ is a flat $SL(2)$ -connection in a bundle E , to say that we diagonalize ∇ locally is to say that we decompose E locally as a direct sum of two ∇ -invariant bundles, i.e. we write locally $E \simeq \mathcal{L}_1 \oplus \mathcal{L}_2$, and ∇ restricts to give a connection in each of the line bundles \mathcal{L}_1 and \mathcal{L}_2 . However, as we have mentioned, our abelian gauge jumps by a permutation matrix at branch cuts. A more intrinsic and global way to say this, avoiding any particular choice of cuts, is that rather than two independent and locally defined bundles \mathcal{L}_1 and \mathcal{L}_2 with flat connections, what we really have is a single line bundle \mathcal{L} over the covering space Σ , again carrying a flat connection ∇^{ab} . Our abelian gauge should then be understood as an isomorphism $\iota : E \simeq \pi_* \mathcal{L}$ which takes ∇ to $\pi_* \nabla^{\text{ab}}$.

Now we can give the precise definition. Let ∇ be a flat $SL(2)$ -connection in a bundle E , and \mathcal{W} a spectral network subordinate to the covering Σ . A \mathcal{W} -abelianization of ∇ is:

- a complex line bundle \mathcal{L} over Σ ,
- an isomorphism $\iota : E \simeq \pi_* \mathcal{L}$ defined on $C \setminus \mathcal{W}$,
- a connection ∇^{ab} in \mathcal{L} , defined on $\pi^{-1}(C \setminus \mathcal{W})$,

obeying the conditions that

- when restricted to $C \setminus \mathcal{W}$, the isomorphism ι takes ∇ to $\pi_* \nabla^{\text{ab}}$,
- ι jumps by a map $S_w = 1 + e_w \in \text{End}(\pi_* \mathcal{L})$ at each wall $w \subset \mathcal{W}$, where $e_w : \mathcal{L}_i \rightarrow \mathcal{L}_j$ if w carries the label ij . (In local coordinates this just says S_w is upper or lower triangular according to the label ij .)

4.2 Properties of abelianization

We have now defined what we mean by a \mathcal{W} -abelianization of ∇ . In the following sections we will see how to construct \mathcal{W} -abelianizations concretely, for various different \mathcal{W} . First, though, let us explore a bit more thoroughly the expected properties of the corresponding connections ∇^{ab} .

First, although it was defined a priori only away from \mathcal{W} , ∇^{ab} extends continuously over \mathcal{W} . Indeed, consider a single wall carrying the label (say) 21. Choosing a local trivialization of \mathcal{L} in some neighborhood of the wall, $\pi_* \mathcal{L}$ also becomes trivial there. Thus ι amounts to two bases (s_1, s_2) and (s'_1, s'_2) for E , related by an upper-triangular transformation, i.e. $s'_1 = s_1$ and $s'_2 = s_2 + \alpha s_1$ for some function α . These bases diagonalize the connection ∇ , we have $\nabla s_1 = d_1 s_1$ and $\nabla s_2 = d_2 s_2$ on one side of the wall, and on the other side $\nabla s'_1 = d'_1 s'_1$ and $\nabla s'_2 = d'_2 s'_2$. First, note that since $s'_1 = s_1$ it follows immediately that $d'_1 = d_1$. Now $\nabla s'_2 = \nabla(s_2 + \alpha s_1) = \nabla^{\text{ab}} s_2 + (d\alpha) s_1 + \alpha \nabla^{\text{ab}} s_1$. On the other hand $\nabla s'_2 = d'_2 s'_2 = d'_2 (s_2 + \alpha s_1)$. Comparing these two results gives $d'_2 = d_2$ (and $d\alpha = (d_2 - d_1)\alpha$.) Summing up, we have $d_1 = d'_1$ and $d_2 = d'_2$. But the connection $\pi_* \nabla^{\text{ab}}$ is represented (in our local trivialization) exactly by the diagonal matrices $\text{diag}(d_1, d_2)$ and $\text{diag}(d'_1, d'_2)$ on the two sides of the wall. Thus our result says precisely that ∇^{ab} extends continuously across the wall.

It is then interesting to ask whether ∇^{ab} can also be extended over the branch points, to give a connection over the whole of Σ . To check this, it suffices to compute the holonomy

of ∇^{ab} around a single branch point. This turns out to be easy: since ∇ is an $SL(2, \mathbb{C})$ connection, $\pi_* \nabla^{\text{ab}}$ must be as well, and so the holonomy of $\pi_* \nabla^{\text{ab}}$ around the branch point on C is of the form

$$\begin{pmatrix} 0 & D \\ -D^{-1} & 0 \end{pmatrix}.$$

Going twice around the branch point on C then gives

$$\begin{pmatrix} 0 & D \\ -D^{-1} & 0 \end{pmatrix}^2 = \begin{pmatrix} -1 & 0 \\ 0 & -1 \end{pmatrix} \quad (4.1)$$

for the holonomy of $\pi_* \nabla^{\text{ab}}$, which says that the holonomy of ∇^{ab} around the branch point on Σ is -1 . Thus ∇^{ab} cannot be extended over the branch points, but its failure to extend is completely under control. We refer to a connection ∇^{ab} with this property as an *almost-flat* connection over Σ .

The connection ∇^{ab} also comes with some extra structure, as follows. The fact that ∇ is an $SL(2, \mathbb{C})$ connection means that the underlying bundle E carries a ∇ -invariant, nonvanishing volume form $\varepsilon_E \in \wedge^2(E)$. Now suppose we locally label the sheets of Σ . Then we get a ∇^{ab} -invariant pairing $\mathcal{L}_1 \otimes \mathcal{L}_2 \rightarrow \mathbb{C}$, defined by $(s_1, s_2) \mapsto (s_1 \wedge s_2) / \varepsilon_E$. This gives a ∇^{ab} -invariant isomorphism $\rho : \mathcal{L}_1 \simeq \mathcal{L}_2^*$. To describe this globally, we introduce the automorphism $\sigma : \Sigma \rightarrow \Sigma$ which exchanges the two sheets. Then what we have is a ∇^{ab} -invariant isomorphism ρ between \mathcal{L} and $(\sigma^* \mathcal{L})^*$. We call a connection equipped with such an isomorphism *equivariant*.

What we have shown is that the connections ∇^{ab} which arise in \mathcal{W} -abelianization automatically carry some extra structure: they are defined on the complement of the branch locus in Σ , and they are almost-flat and equivariant.

4.3 Equivalence of abelianizations

If we have a flat $SL(2)$ -connection ∇ and a \mathcal{W} -abelianization $(\mathcal{L}, \iota, \nabla^{\text{ab}})$ of ∇ , we can easily generate other \mathcal{W} -abelianizations of ∇ . Indeed, let $\mu : \Sigma \rightarrow \mathbb{C}^\times$ be any function; then multiplication by μ gives an automorphism of \mathcal{L} and of $\pi_* \mathcal{L}$, and $(\mathcal{L}, \iota \circ \mu, \mu^* \nabla^{\text{ab}})$ is another \mathcal{W} -abelianization of ∇ . One could say loosely that these two \mathcal{W} -abelianizations just differ by a diagonal gauge transformation. We call two \mathcal{W} -abelianizations which are related in this way *gauge equivalent*. If two \mathcal{W} -abelianizations of ∇ are gauge equivalent, in particular the corresponding connections ∇^{ab} are equivalent.

4.4 Spectral coordinates

So far we have explained what we mean by \mathcal{W} -abelianization. It is a certain relation between a flat $SL(2, \mathbb{C})$ -connection ∇ over C and an almost-flat equivariant \mathbb{C}^\times -connection ∇^{ab} over Σ .

Given an almost-flat equivariant \mathbb{C}^\times -connection ∇^{ab} we can construct some interesting numbers, as follows. Let Σ' denote Σ with the branch points removed. Given any class $\gamma \in H_1(\Sigma', \mathbb{Z})$ we can consider the holonomy

$$\mathcal{X}_\gamma = \text{Hol}_\gamma \nabla^{\text{ab}} \in \mathbb{C}^\times. \quad (4.2)$$

From their definition it immediately follows that they are multiplicative:

$$\mathcal{X}_\gamma \mathcal{X}_{\gamma'} = \mathcal{X}_{\gamma+\gamma'}. \quad (4.3)$$

Moreover, if γ_b denotes a loop around a branch point, then we have

$$\mathcal{X}_{\gamma_b} = -1. \quad (4.4)$$

Finally, the equivariance of ∇^{ab} implies a further relation:

$$\mathcal{X}_{\gamma+\sigma_*\gamma} = 1. \quad (4.5)$$

It follows from (4.3), (4.4), (4.5) that if we fix a collection $\{\gamma_i\} \subset H_1(\Sigma', \mathbb{Z})$ such that their images in $H_1(\Sigma, \mathbb{Z}) / \langle \gamma + \sigma_*\gamma \rangle$ form a basis, then the \mathcal{X}_{γ_i} are enough to determine all of the \mathcal{X}_γ .

Below we will see that for many examples of \mathcal{W} , there exist just finitely many different ways of \mathcal{W} -abelianizing a generic connection ∇ . To pick out exactly one \mathcal{W} -abelianization, we will need a bit of extra structure which we call a \mathcal{W} -framing of ∇ . Given a \mathcal{W} -framed connection ∇ we will see that there is a really canonical way of \mathcal{W} -abelianizing it to obtain a connection ∇^{ab} . Thus the numbers \mathcal{X}_{γ_i} , which a priori depend on ∇^{ab} , can be thought of as functions of the \mathcal{W} -framed connection ∇ . Thus they are functions on the moduli space of \mathcal{W} -framed flat $SL(2)$ -connections, and in fact we will be able to construct coordinate systems on this moduli space in this way. Thus we call the \mathcal{X}_{γ_i} *spectral coordinates*.

Spectral coordinate systems have some nice properties which distinguish them from arbitrary coordinate systems. In particular, it was shown in [1] that they are actually *Darboux* coordinates in the following sense. The moduli space of flat connections over C has a natural holomorphic Poisson structure, described e.g. in [21] (generalizing the symplectic structure which one gets when C is closed [22]). The functions \mathcal{X}_γ have simple Poisson brackets with respect to this structure:

$$\{\mathcal{X}_\gamma, \mathcal{X}_{\gamma'}\} = \langle \gamma, \gamma' \rangle \mathcal{X}_{\gamma+\gamma'}, \quad (4.6)$$

where $\langle \cdot, \cdot \rangle$ denotes the intersection pairing on $H_1(\Sigma', \mathbb{Z})$. In particular, if we fix our basis $\{\gamma_i\}$ so that the intersection pairing is of the block form

$$\begin{pmatrix} 0 & 1 & 0 \\ -1 & 0 & 0 \\ 0 & 0 & 0 \end{pmatrix},$$

the corresponding spectral coordinates consist of Darboux coordinates for the symplectic leaves of the moduli space plus functions in the Poisson center.

4.5 Fock-Goncharov spectral networks

Suppose we are given a Fock-Goncharov network \mathcal{W} and a flat $SL(2)$ -connection ∇ on C . How do we \mathcal{W} -abelianize ∇ ? As we will now see, this can be done, but not quite for every ∇ , and not quite uniquely. To get a unique abelianization, we should equip ∇

with a bit of extra structure. Given a flat $SL(2)$ -connection ∇ and a puncture z_i on C , let a *framing* of ∇ at z_i be a choice of a 1-dimensional eigenspace ℓ of the monodromy of ∇ around z_i . We define a \mathcal{W} -framed connection to be a flat $SL(2)$ -connection ∇ plus a choice of a framing around each puncture, subject to an additional condition: if two punctures z_i, z_j can be connected by a path which does not meet \mathcal{W} , then if we parallel transport the framing from z_i to z_j along this path, the line we get is distinct from the framing at z_j . This condition is automatically satisfied for a generic ∇ . Moreover, for generic ∇ , the choice of a \mathcal{W} -framing is a discrete choice: the monodromy around each puncture has two distinct eigenspaces, and we are just choosing one of them. What we will show below is that there is a canonical \mathcal{W} -abelianization of any \mathcal{W} -framed connection.

Let \mathcal{L} be the trivial bundle over Σ . Our \mathcal{W} -abelianization of ∇ will be determined by giving an isomorphism $\iota : E \simeq \pi_*\mathcal{L}$ over $C \setminus \mathcal{W}$. $C \setminus \mathcal{W}$ consists of “cells” with the topology of component (1) in Figure 3; let c denote one such cell.

Suppose we label the sheets over c by 1 and 2.⁶ Giving ι over c is then equivalent to giving a basis (s_1, s_2) of E over c . How will we get this basis? On the boundary of c we have two punctures, each carrying a decoration. Moreover, our rules for spectral networks imply that the two decorations are opposite: thus one puncture is labeled 12 (call this puncture z_1) and the other 21 (call this puncture z_2).⁷ Each puncture has a framing; call these ℓ_1 and ℓ_2 . By parallel transporting the framings ℓ_1 and ℓ_2 to a general $z \in c$, we obtain lines $\ell_1(z)$ and $\ell_2(z)$ in E_z . Our basis (s_1, s_2) will be obtained by choosing $s_1(z) \in \ell_1(z)$ and $s_2(z) \in \ell_2(z)$. Crucially, for any such choice, ∇ is diagonal relative to the basis (s_1, s_2) ; this says exactly that ∇ corresponds to a connection ∇^{ab} in the line bundle \mathcal{L} .

Note that this construction would have failed if $\ell_1(z) = \ell_2(z)$, since in that case $s_1(z)$ and $s_2(z)$ are not linearly independent, so they do not form a basis of E_z . This is why we required that $\ell_1(z) \neq \ell_2(z)$ in the definition of \mathcal{W} -framed connection.

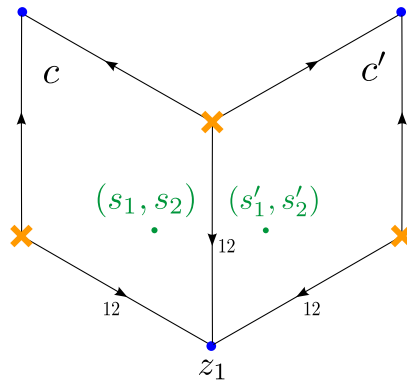


Figure 19: Bases (s_1, s_2) and (s'_1, s'_2) attached to the two sides of a wall that separates the cells c and c' .

⁶We emphasize that this is only a *local* labeling; it would not be possible to give such a labeling globally without branch cuts, but we can always do it over c since c is simply connected. Thus in what follows we will not have to worry about branch cuts.

⁷The decoration at the puncture thus determines whether the eigensection s at that puncture is associated to the first or second sheet of the cover.

Now let us consider the change-of-basis matrix S_w . Consider the two bases (s_1, s_2) and (s'_1, s'_2) attached to the two sides of the wall in Figure 19. Because the two cells c, c' have the vertex z_1 in common, we will have $\ell_1 = \ell'_1$, so s_1 and s'_1 can differ at most by scalar multiple. This implies that the transformation S_w taking (s_1, s_2) to (s'_1, s'_2) has the form

$$S_w = \begin{pmatrix} * & * \\ 0 & * \end{pmatrix}$$

relative to the basis (s_1, s_2) . By a diagonal “gauge transformation” of the form

$$(s'_1(z), s'_2(z)) \mapsto (\lambda_1(z)s'_1(z), \lambda_2(z)s'_2(z)), \quad (4.7)$$

where λ_1 and λ_2 are functions on c' , we can thus arrange that

$$S_w = \begin{pmatrix} 1 & * \\ 0 & 1 \end{pmatrix} \quad (4.8)$$

relative to the basis (s_1, s_2) . This is the desired form for the jump of ι according to the definition of abelianization.

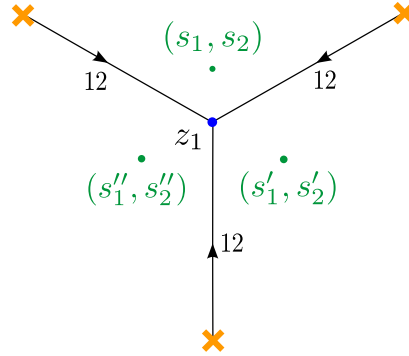


Figure 20: Neighborhood of a puncture with bases.

We have now described how a \mathcal{W} -framed connection ∇ can be \mathcal{W} -abelianized. Moreover this abelianization is essentially unique, as we will now explain. Suppose we have *any* \mathcal{W} -abelianization of the connection ∇ . Consider a neighborhood of a puncture z_1 as shown in Figure 20. In each cell, our \mathcal{W} -abelianization gives a pair of sections $s_1(z), s_2(z)$, with respect to which ∇ is diagonal. The constraint that S_w is of the form (4.8) says that at S_w preserves s_1 , i.e. along the wall w we have $s_1(z) = s'_1(z)$. Continuing around the wall we see that s_1, s'_1, s''_1 are the restrictions of a single section $\hat{s}_1(z)$ defined in a whole neighborhood of the puncture, such that $\nabla \hat{s}_1(z)$ is a multiple of $\hat{s}_1(z)$. In other words $\hat{s}_1(z)$ is an eigenvector of the monodromy of ∇ around the puncture.

Applying this condition to every puncture almost determines our local bases. Let us consider the choices remaining. First, there is the choice of *which* eigenvector to take at each puncture: this is the choice we have incorporated into our definition of \mathcal{W} -framed connection. Second, there is the freedom to make an overall rescaling $(s_1(z), s_2(z)) \rightarrow (\lambda_1(z)s_1(z), \lambda_2(z)s_2(z))$ in each cell (matching up along the walls). Such a change gives a

gauge equivalent \mathcal{W} -abelianization. In particular, it changes the connection ∇^{ab} only by a $GL(1)$ -gauge transformation.

Finally, let us see how to compute the spectral coordinates of a given connection ∇ . Consider the cycle γ on Σ' shown in Figure 21.

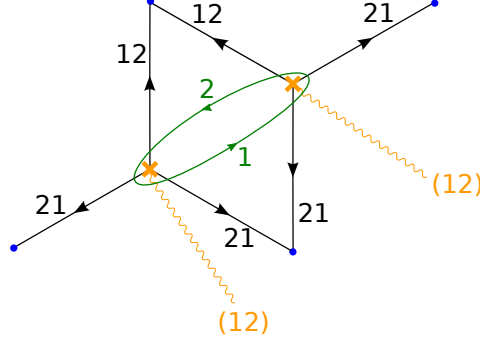


Figure 21: Cycle γ in a quadrilateral Q , with vertices at the four punctures.

To compute \mathcal{X}_γ we first consider a more basic object. Take a single branch point and its three associated punctures, and a path a on Σ as shown in Figure 22. We aim to describe

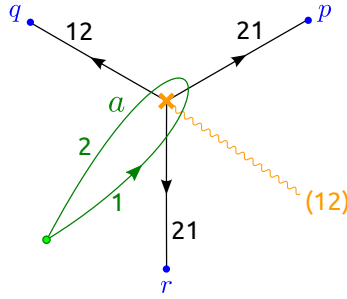


Figure 22: Path a around a branch point.

how the parallel transport of ∇^{ab} along a acts; call this parallel transport \mathcal{X}_a for short.

Let s_q denote some section of ℓ_q , and similarly for the other punctures. Since a is a path beginning on sheet 1 of Σ and ending on sheet 2, we have

$$\mathcal{X}_a(s_r) = \lambda s_q \quad (4.9)$$

for some scalar λ . Our job is to determine λ . For this, divide a into three segments $a = a_1 a_2 a_3$, each crossing one of the walls. Using $\mathcal{X}_a = \mathcal{X}_{a_3} \mathcal{X}_{a_2} \mathcal{X}_{a_1}$, (4.9) becomes

$$\mathcal{X}_{a_2} \mathcal{X}_{a_1}(s_r) = \lambda \mathcal{X}_{a_3}^{-1} s_q. \quad (4.10)$$

The triangular structure of the S_w says that we have $\mathcal{X}_{a_1}(s_r) = s_r$, $\mathcal{X}_{a_3}(s_q) = s_q$, so that we can simplify (4.10) to

$$\mathcal{X}_{a_2}(s_r) = \lambda s_q. \quad (4.11)$$

The triangular structure of the S_w also says $(\mathcal{X}_{a_2}(s_r) - s_r) \sim s_p$, which means $(\mathcal{X}_{a_2}(s_r) - s_r) \wedge s_p = 0$, i.e.

$$\lambda = \frac{s_r \wedge s_p}{s_q \wedge s_p}. \quad (4.12)$$

Now consider two neighboring branch points, as in Figure 23. The previous analysis

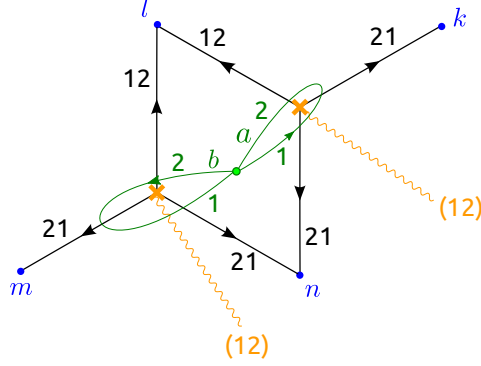


Figure 23: Cycle $\gamma = a + b$ in the quadrilateral Q with vertices k, l, m and n .

shows that

$$\mathcal{X}_a(s_n) = \frac{s_n \wedge s_k}{s_l \wedge s_k} s_l, \quad \mathcal{X}_b(s_l) = \frac{s_l \wedge s_m}{s_n \wedge s_m} s_n. \quad (4.13)$$

Combining these gives

$$\mathcal{X}_a \mathcal{X}_b(s_l) = \frac{s_n \wedge s_k}{s_l \wedge s_k} \frac{s_l \wedge s_m}{s_n \wedge s_m} s_l, \quad (4.14)$$

but $a + b = \gamma$, so finally we can write the holonomy along the closed cycle γ :

$$\mathcal{X}_\gamma = \frac{(s_n \wedge s_k)(s_l \wedge s_m)}{(s_l \wedge s_k)(s_n \wedge s_m)}. \quad (4.15)$$

We emphasize that the expression (4.15) for \mathcal{X}_γ is $SL(2)$ invariant, and can thus be evaluated at any internal point of the quadrilateral Q . This is the main result of this section: it gives a concrete formula for the spectral coordinates in terms of data attached to the original $SL(2)$ connection ∇ .

This formula is a familiar one. Indeed, consider the ideal triangulation \mathcal{T} which corresponds to the Fock-Goncharov network \mathcal{W} . The quadrilateral Q contains a unique edge of this triangulation. On the other hand, for each edge of \mathcal{T} there is a corresponding ‘‘complexified shear coordinate’’ or ‘‘Fock-Goncharov coordinate’’ on the space of \mathcal{W} -framed connections [9]. Thus, to the quadrilateral Q we could associate a corresponding Fock-Goncharov coordinate. Up to a minus sign, \mathcal{X}_γ given by (4.15) is exactly that coordinate. (The sign discrepancy can be eliminated by shifting γ by a loop around a branch point, i.e. replacing γ by γ' shown in Figure 24.)

Applying this result to each cell in turn, we obtain a collection of cycles $\gamma_i \in H_1(\Sigma, \mathbb{Z})$ such that the spectral coordinates \mathcal{X}_{γ_i} are exactly the Fock-Goncharov coordinates attached to the ideal triangulation \mathcal{T} . We have thus rederived the result of [4] in the special

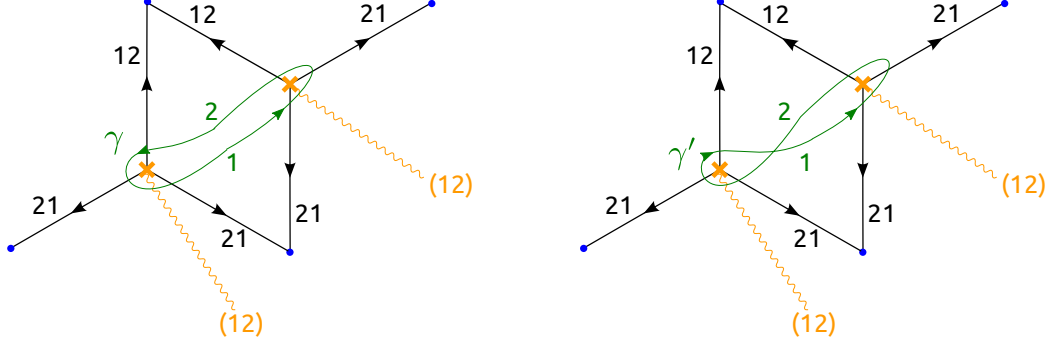


Figure 24: The homology classes γ and γ' differ only by the addition of a loop around one of the branch points on Σ . Thus $\mathcal{X}_{\gamma'} = -\mathcal{X}_{\gamma}$.

case $K = 2$ (see also [3] where essentially the same result appeared, albeit phrased in a different language.)

In general, knowing the \mathcal{X}_{γ_i} does not quite determine all of the spectral coordinates. Indeed, the cycles γ_i descend to a \mathbb{Q} -basis for $H_1(\Sigma, \mathbb{Q})/\langle \gamma + \sigma_*\gamma \rangle$, but not to a \mathbb{Z} -basis. Thus the spectral coordinates contain slightly more information than the Fock-Goncharov coordinates. It seems that this extra information is enough to determine the full $SL(2)$ -connection ∇ (up to gauge equivalence), whereas the Fock-Goncharov coordinates would be enough to determine only its projection to $PSL(2)$. We will not give a general proof of this here, but we will see how it works explicitly in the examples in §6.

4.6 Fenchel-Nielsen spectral networks

Next suppose we are given a Fenchel-Nielsen spectral network \mathcal{W} and a flat $SL(2)$ -connection ∇ over C .

As for Fock-Goncharov networks, we need to enrich ∇ by some extra data in order to get a canonical \mathcal{W} -abelianization, as follows. The complement $C' = C \setminus \mathcal{W}$ consists of various connected components A , each with the topology of an annulus. There are two ways of going around the annulus; define a *framing* of ∇ on A to be a 1-dimensional eigenspace of the monodromy in each direction (so if we label the two directions $+$ and $-$, then we give an eigenspace ℓ_+ of the monodromy M_+ and an eigenspace ℓ_- of the monodromy $M_- = M_+^{-1}$.) We require that these two lines are distinct, $\ell_+ \neq \ell_-$, and also that the lines ℓ_{\pm} for any annulus are distinct from the lines ℓ_{\pm} for any adjacent annulus.⁸ Note that a framing of ∇ on A exists only if M_{\pm} are diagonalizable. Finally, we define a \mathcal{W} -framed connection to be a flat $SL(2)$ -connection ∇ plus a framing of ∇ on each annulus A .

We can now proceed much as we did for the Fock-Goncharov networks. Fix an annulus A . By parallel transport, the framing of ∇ on A gives two lines $\ell_+(z) \subset E_z$ and

⁸This last constraint is equivalent to ∇ being irreducible when restricted to any pair of pants. Indeed, suppose that two lines are equal for adjacent annuli. Consider any pair of pants that has the two adjacent annuli as boundary components. The third annulus then also needs to carry the same line. This implies that the representation is reducible when restricted to this pair of pants.

$\ell_-(z) \subset E_z$ (note that this makes global sense over A only because ℓ_{\pm} are monodromy eigenspaces.) Choose a section $s_+(z)$ valued in $\ell_+(z)$ and a section $s_-(z)$ valued in $\ell_-(z)$. We want to use this pair of sections to build an isomorphism $\iota : E \rightarrow \pi_*\mathcal{L}$, where \mathcal{L} denotes the trivial bundle over Σ . Concretely, the covering Σ is trivializable over A , so we may choose a labeling of the sheets by 1 and 2; after so doing, what we need to do is to choose which of s_{\pm} will be s_1 and which will be s_2 . This extra information is provided by the decoration of \mathcal{W} on A : if the labeling attached to the $+$ direction is ij , then we take $s_i = s_+$ and $s_j = s_-$.

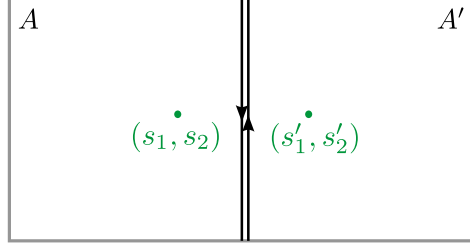


Figure 25: Bases of sections on either side of a double wall that separates two annuli A and A' . (For a global picture see e.g. Figure 6.)

Now we need to arrange that the change-of-basis matrices S_w attached to the walls $w \subset \mathcal{W}$ are of the required triangular form. Consider the double wall shown in Figure 25, separating annuli A, A' . What we require is that the matrix taking (s_1, s_2) to (s'_1, s'_2) , relative to the basis (s_1, s_2) , is of the form

$$\begin{pmatrix} 1 & 0 \\ * & 1 \end{pmatrix} \begin{pmatrix} 1 & * \\ 0 & 1 \end{pmatrix} \quad (4.16)$$

This is a rather weak requirement: it just says that this matrix has determinant 1 and its upper left entry is 1. Since s'_1 and s_2 are not proportional, and s'_2 and s_1 are not proportional, we know at least that neither of the diagonal entries vanishes; thus we can arrange the desired form (4.16) by a rescaling of the form $(s'_1, s'_2) \rightarrow (\lambda_1(z)s'_1, \lambda_2(z)s'_2)$.

Now let us see how to compute the spectral coordinates of a given connection ∇ . Unlike the Fock-Goncharov case, a Fenchel-Nielsen network is not quite enough to determine a canonical basis for $H_1(\Sigma, \mathbb{Z}) / \langle \gamma + \sigma_*\gamma \rangle$. Instead, half of the cycles are canonical (and will be associated to the Fenchel-Nielsen length coordinates, which are likewise canonical) while the other half are not quite canonically defined (and will be associated to the Fenchel-Nielsen twist coordinates, which are likewise known to suffer from some ambiguities.)

Consider the annulus A pictured in Figure 26, and the path \wp going around in the same direction as the walls on the boundary (call this the $+$ direction). We choose a labeling of the sheets of Σ over A , such that the boundary walls are of type ij . Now, let γ be the lift of \wp to sheet j . By definition, the holonomy \mathcal{X}_γ of ∇^{ab} along γ is equal to the eigenvalue of M_+ acting on the section s_j . According to our rules above, $s_j = s_+$. Thus \mathcal{X}_γ is identified with the holonomy eigenvalue corresponding to the section s_+ . This holonomy eigenvalue is a complexified version of a square-root of the exponentiated

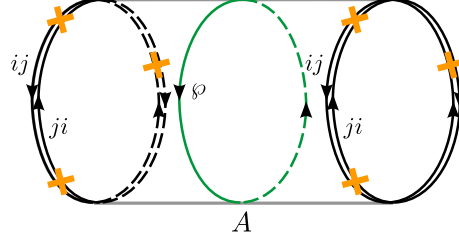


Figure 26: Cycle φ used to compute the spectral length coordinate. (The double walls may contain any positive number of branch points. They could also be replaced by boundary components.)

Fenchel-Nielsen length coordinate. Thus we have found that these length coordinates occur as examples of spectral coordinates.

We might similarly have considered the lift γ' of φ to sheet i ; then by the same reasoning we would have found that $\mathcal{X}_{\gamma'}$ is the holonomy eigenvalue corresponding to s_- . These two eigenvalues are inverse to one another, so we have $\mathcal{X}_{\gamma}\mathcal{X}_{\gamma'} = 1$. This is just as we expect from the equivariance of the connection ∇^{ab} .

The cycles obtained in this way do not descend to a basis of $H_1(\Sigma, \mathbb{Z})$, reflecting the fact that the exponentiated Fenchel-Nielsen length coordinates do not give a complete coordinate system on the moduli of flat $SL(2, \mathbb{C})$ -connections. To get more cycles we can consider ones which cross the annulus A , such as γ pictured in Figure 27.

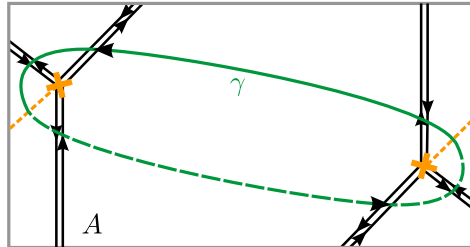


Figure 27: Local region of annulus A intersected by the projection of the cycle γ that is used to define the spectral twist coordinate. The cycle crosses the annulus A in either direction, while winding around two branch points.

How should we understand the coordinate \mathcal{X}_{γ} ? Rather than trying to compute it directly, let us take a slightly more indirect route: we want to consider how \mathcal{X}_{γ} is transformed under a certain modification of the connection ∇ , as follows. Suppose we cut the surface C into two pieces along the annulus A . We will obtain two surfaces with boundary, say C_1 and C_2 , carrying connections ∇_1 and ∇_2 , as well as an isomorphism $i : E_1 \simeq E_2$ along the boundary, with $\nabla_1 = i^*\nabla_2$. We could now glue C back together along the boundary using the isomorphism i to recover the original ∇ . However, we could instead glue with an isomorphism $i' = i \circ a$, where a is any automorphism of E_1 which preserves ∇_1 . Such an automorphism must preserve the monodromy eigenspaces: thus, in terms of the sections s_1, s_2 of E over A , the action of a can be written as $s_1 \rightarrow \lambda s_1, s_2 \rightarrow \lambda^{-1} s_2$. Thus we obtain a 1-parameter family of modified connections $\nabla(\lambda)$. This

operation is sometimes called the “twist flow.”

If the original connection ∇ was abelianized by ∇^{ab} , then $\nabla(\lambda)$ is also abelianized by a connection $\nabla^{\text{ab}}(\lambda)$, constructed by the abelian version of the twist flow: we cut Σ apart along two preimages of A , then reglue using the automorphism $s \rightarrow \lambda s$ on sheet 1 and $s \rightarrow \lambda^{-1}s$ on sheet 2. From this description, it follows the twist flow acts rather simply on the coordinate \mathcal{X}_γ :

$$\mathcal{X}_\gamma \rightarrow \lambda^2 \mathcal{X}_\gamma. \quad (4.17)$$

One sees this by directly computing the parallel transport of $\nabla^{\text{ab}}(\lambda)$ along γ : it is identical to that of ∇^{ab} , except for two extra factors of λ for the two times the path γ crosses the annulus.

The property (4.17) is enough to determine \mathcal{X}_γ up to a multiplicative constant. Moreover, it allows us to recognize \mathcal{X}_γ as a well-studied object: indeed, any function on the moduli space of connections ∇ which transforms by (4.17) under the twist flow is known as a “Fenchel-Nielsen twist coordinate.” We call it *a* twist coordinate rather than *the* twist coordinate because of the ambiguity just mentioned. To fix this ambiguity one needs some further choice beyond that of a pants decomposition. What we have seen here is that given a particular Fenchel-Nielsen network \mathcal{W} and a particular choice of a cycle γ crossing the annulus, the spectral coordinate \mathcal{X}_γ is a particular Fenchel-Nielsen twist coordinate. Changing the choice of γ while keeping the network \mathcal{W} fixed evidently multiplies the twist coordinate \mathcal{X}_γ by a power of the exponentiated length coordinate.

So far we have found that the Fenchel-Nielsen length and twist coordinates can be obtained as spectral coordinates associated to the Fenchel-Nielsen network \mathcal{W} . Actually, the spectral coordinates contain slightly more information than the Fenchel-Nielsen coordinates. Indeed, the exponentiated Fenchel-Nielsen length coordinate is equal to the *square* of the spectral coordinate \mathcal{X}_γ . Whereas the spectral coordinates determine the full $SL(2)$ connection (up to gauge equivalence), the Fenchel-Nielsen coordinates determine only its projection to $PSL(2)$. We will see how this works explicitly in the examples in §6.

4.7 Trivialization at boundary components

It is sometimes useful to consider the moduli space $\widetilde{\mathcal{M}}$ of \mathcal{W} -framed flat connections with a fixed trivialization at the boundary. More precisely, we choose a trivialization at a marked point of every boundary component of C .

The fixed trivializations are for instance convenient for considering the gluing of two surfaces C and C' along a common boundary component B . The moduli space of flat connections with fixed trivialization on the glued surface $\widetilde{C} = C \cup_B C'$ is equal to

$$\widetilde{\mathcal{M}}_{\widetilde{C}} = \left(\widetilde{\mathcal{M}}_C \times \widetilde{\mathcal{M}}_{C'} \right) / G, \quad (4.18)$$

where G is the group of diagonal gauge transformations at the marked point on B . See Figure 28 for a local picture of the gluing.

When we fix a trivialization at the boundary, we can apply the abelianization procedure much as before; the corresponding flat connections ∇^{ab} will also have fixed trivializations at the boundary. Thus the abelian flat connection up to equivalence is no longer

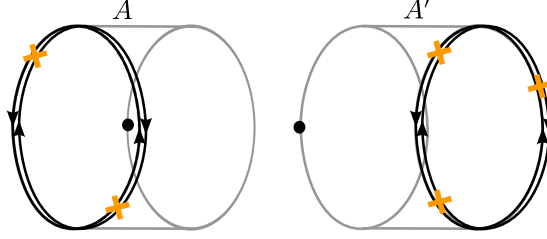


Figure 28: Local picture in which two boundary components A and A' are glued. The marked point on each boundary component is indicated as a black dot.

determined by spectral coordinates attached to a basis of closed 1-cycles on Σ ; rather, the spectral coordinates are attached to a basis of the relative homology $H_1(\Sigma, \partial\Sigma, \mathbb{Z})$. Note that abelianization commutes with gluing.

4.8 Mixed spectral networks

In the last two sections we have described the process of \mathcal{W} -abelianization when \mathcal{W} is a Fock-Goncharov or a Fenchel-Nielsen network. More generally we might take \mathcal{W} to be a mixed spectral network. Such networks lie somewhere between the two extremes just considered. We can still carry out the \mathcal{W} -abelianization process when \mathcal{W} is mixed; indeed, all of our considerations were *local*, involving just a particular cell or a particular (single or double) wall. Each cell of $C \setminus \mathcal{W}$ has one of the two topologies we have just dealt with above, so we can determine the abelianization on each cell using the same recipes we used above. Moreover, by appropriate rescalings of the sections (s_1, s_2) on each cell, we will be able to arrange the desired form for the change-of-basis matrices S_w at each wall, just as we did above.

We expect that the corresponding spectral coordinate system is a kind of hybrid between Fock-Goncharov and Fenchel-Nielsen, containing some coordinates of each kind along with novel types of coordinates.

5 Nonabelianization

In the last section we described how \mathcal{W} -abelianization defines Darboux coordinates on the moduli space of flat $SL(2)$ connections on C . When we reduce from $SL(2)$ to $PSL(2)$ connections, moreover, we found that the spectral coordinates for Fock-Goncharov networks are complex shear coordinates and for Fenchel-Nielsen networks are complex length-twist coordinates. To see more explicitly how this works in practice, in this section we consider the inverse of the abelianization map, the *nonabelianization* map. This map was described in [1]; here we will describe it in a more explicit way.

Given a spectral network \mathcal{W} , the nonabelianization map $\Psi_{\mathcal{W}}$ takes equivariant almost-flat \mathbb{C}^\times -connections ∇^{ab} over Σ to $SL(2)$ -connections $\nabla = \Psi_{\mathcal{W}}(\nabla^{\text{ab}})$ over C . The advantage of this perspective is that it systematically produces flat $SL(2)$ connections in terms of the spectral data. Moreover, it gives a natural interpretation to the unipotent transfor-

mations S_w that we encountered in the last section. In the next section we will apply the nonabelianization procedure for various examples of spectral networks.

5.1 Almost-flat equivariant abelian representations

Instead of working with flat connections, in what follows we will work directly with the corresponding integrated objects, i.e. with their parallel transport matrices. Thus we first define the notion of “almost-flat equivariant abelian representation” on Σ . Almost-flat equivariant abelian representations correspond to the equivariant almost-flat abelian connections ∇^{ab} which we discussed in the last section. We will obtain them as $GL(1)$ -representations ρ^{ab} of a groupoid $\mathcal{G}_{\Sigma'}$ of paths on Σ' . Likewise, we think of flat $SL(2)$ connections on C as $SL(2)$ -representations ρ of groupoid \mathcal{G}_C of paths on C .

Path groupoids

We construct the path groupoids \mathcal{G}_C and $\mathcal{G}_{\Sigma'}$ as follows.

First we fix a set \mathcal{P}_C of marked *basepoints* on C . We choose a basepoint z_w along each wall w , and a basepoint z_b for each boundary component of C . The nonabelianization map will not depend on the choices we make here.

We define the groupoid \mathcal{G}_C to consist of all paths \wp which begin and end at points of \mathcal{P}_C , up to homotopy. We call a path in \mathcal{G}_C *short* if it does not cross any walls in its interior and choose a set of generators \wp_n for \mathcal{G}_C that consists of only short paths. See Figure 29 for an example.

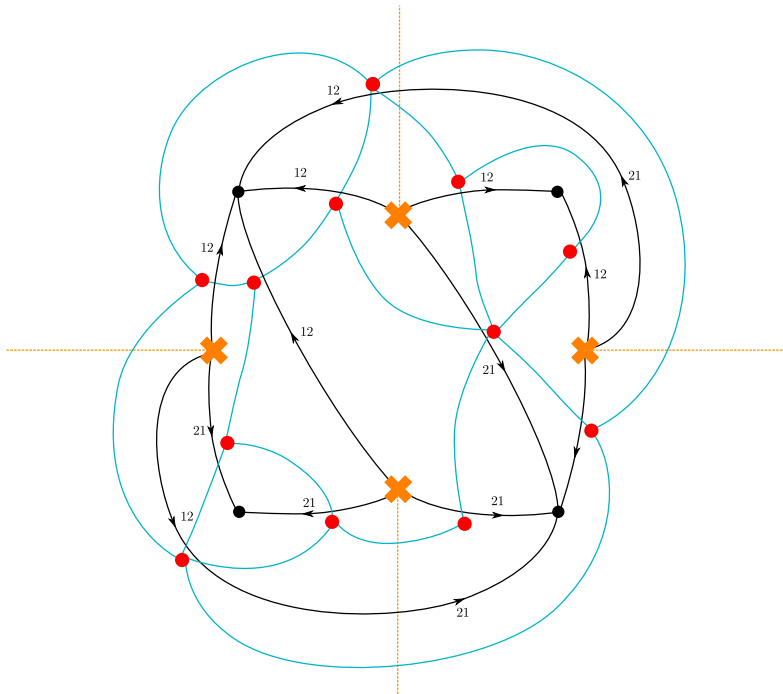


Figure 29: Example of a configuration of basepoints (red dots) and short paths (light blue lines) for a Fock-Goncharov network on the four-punctured sphere.

On the cover Σ we consider the set $\mathcal{P}_{\Sigma'}$ of basepoints that consists of all preimages of basepoints on C , i.e. for each $z \in \mathcal{P}_C$ we have two elements $z^{(i)} \in \mathcal{P}_{\Sigma'}$. We write a generic element in the fundamental groupoid $\mathcal{G}_{\Sigma'}$ as a lift $\wp^{(ij)}$ of a path $\wp \in \mathcal{G}_C$, where the superscripts i and j denote the sheets where the initial and final points of the lifted path live. We define the groupoid $\mathcal{G}_{\Sigma'}$ to consist of all paths on Σ' that are lifts of paths in \mathcal{G}_C , up to homotopy on Σ' .

Almost-flat equivariant representation ρ^{ab}

Define an *almost-flat equivariant representation on Σ* to be a representation

$$\rho^{\text{ab}} : \mathcal{G}_{\Sigma'} \rightarrow GL(1) \quad (5.1)$$

such that for any $\wp \in \mathcal{G}_C$

$$\rho^{\text{ab}}(\wp^{(i^\sigma j^\sigma)})^{-1} = (-1)^{i+j} \rho^{\text{ab}}(\wp^{(ij)}). \quad (5.2)$$

Almost-flat equivariant representations can be concretely specified by giving their action on generators of $\mathcal{G}_{\Sigma'}$. These generators then must obey the relations of the path groupoid $\mathcal{G}_{\Sigma'}$; we refer to these as the “bulk constraints.” In addition, when γ is a homotopically trivial loop around a branch point, we impose

$$\rho^{\text{ab}}(\gamma) = -1. \quad (5.3)$$

We call these constraints the “branch point constraints.”

Given two almost-flat equivariant representations ρ^{ab} and ρ'^{ab} on Σ , an *equivalence* between ρ^{ab} and ρ'^{ab} is a map $g^{\text{ab}} : \mathcal{P}_{\Sigma'} \rightarrow GL(1)$ such that for all boundary basepoints

$$g^{\text{ab}}(z_b^{(i)}) = 1, \quad (5.4)$$

and for all $\wp \in \mathcal{G}_C$,

$$\rho'^{\text{ab}}(\wp^{(ij)}) = g^{\text{ab}}(z_{i(\wp)}^{(i)}) \rho^{\text{ab}}(\wp^{(ij)}) \left(g^{\text{ab}}\right)^{-1}(z_{f(\wp)}^{(j)}), \quad (5.5)$$

where $i(\wp)$ is the initial point of \wp and $f(\wp)$ its final point.

Constructing ρ^{ab}

To describe an almost-flat equivariant representation ρ^{ab} concretely, it is enough to give elements $\rho^{\text{ab}}(\wp_n^{(ij)}) \in GL(1)$ for all generators $\wp_n^{(ij)}$. It will be convenient to organize these elements into a collection of $SL(2)$ -valued matrices \mathcal{D}_{\wp_n} , which are diagonal if \wp_n does not cross a branch cut and strictly off-diagonal if \wp_n does cross a branch cut. Thus we let

$$\rho^{\text{ab}}(\wp_n^{(ij)}) = (\mathcal{D}_{\wp_n})_{ij}. \quad (5.6)$$

When \wp is a path that is not short, say $\wp = \wp_1\wp_2$, and has a lift $\wp^{(ij)} = \wp_1^{(ik)}\wp_2^{(kj)}$, we have

$$\begin{aligned}\rho^{\text{ab}}(\wp^{(ij)}) &= \rho^{\text{ab}}(\wp_1^{(ik)})\rho^{\text{ab}}(\wp_2^{(kj)}) \\ &= (\mathcal{D}_{\wp_1})_{ik}(\mathcal{D}_{\wp_2})_{kj} \\ &= (\mathcal{D}_{\wp_1}\mathcal{D}_{\wp_2})_{ij}.\end{aligned}$$

There is an obvious extension to longer paths.

Assuming that the \mathcal{D}_{\wp} are chosen in such a way that the bulk constraints are satisfied, ρ^{ab} so constructed is indeed an almost-flat equivariant representation. Indeed, for any $\wp^{(ij)} \in \mathcal{G}_{\Sigma}$,

$$\rho^{\text{ab}}(\wp^{(i^{\sigma}j^{\sigma})})^{-1} = (-1)^{i+j}\rho^{\text{ab}}(\wp^{(ij)}) \quad (5.7)$$

Moreover, consider a small loop γ on Σ which goes once around a branch point. Such an γ can be obtained as the concatenation of six paths on Σ , obtained by lifting six short paths on C , $\wp_1\wp_2\wp_3\wp_1\wp_2\wp_3$ (each path is repeated twice; see Figure 30). $\rho^{\text{ab}}(\gamma)$ is thus the ii component of

$$\left[\begin{pmatrix} D_1 & 0 \\ 0 & D_1^{-1} \end{pmatrix} \begin{pmatrix} D_2 & 0 \\ 0 & D_2^{-1} \end{pmatrix} \begin{pmatrix} 0 & D_3 \\ -D_3^{-1} & 0 \end{pmatrix} \right]^2 = \begin{pmatrix} -1 & 0 \\ 0 & -1 \end{pmatrix}. \quad (5.8)$$

Thus $\rho^{\text{ab}}(\gamma) = -1$.

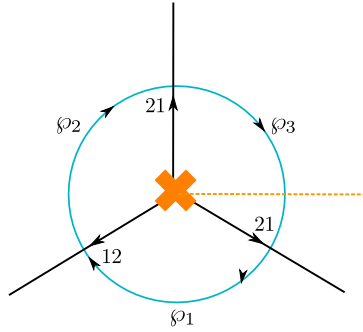


Figure 30: A small loop around a branch point, used to check that ρ^{ab} is almost-flat.

5.2 Nonabelianization map

The nonabelianization map associates to each almost-flat equivariant representation $\rho^{\text{ab}} : \mathcal{G}_{\Sigma'} \rightarrow GL(1)$ a corresponding representation $\rho : \mathcal{G}_C \rightarrow SL(2)$, as follows. The representation ρ^{ab} , as we have just described, can be given in terms of the matrices \mathcal{D}_{\wp} for short paths \wp on C . The corresponding representation ρ will be built from the \mathcal{D}_{\wp} as well, but we will “splice in” some additional unipotent matrices. For each wall w we introduce

a parameter $S_w \in \mathbb{C}$ and a matrix of the form

$$\mathcal{S}_w = \begin{cases} \begin{pmatrix} 1 & S_w \\ 0 & 1 \end{pmatrix} & \text{for } w \text{ of type 21,} \\ \begin{pmatrix} 1 & 0 \\ S_w & 1 \end{pmatrix} & \text{for } w \text{ of type 12.} \end{cases} \quad (5.9)$$

Also fix a normal vector to the wall w (the nonabelianization map ultimately will not depend on this choice.)

Then for any short path $\varphi \in \mathcal{G}_C$, we define $\rho(\varphi)$ to be a product of several matrices,

$$\rho(\varphi) = \mathcal{S}_1 \mathcal{D}_\varphi \mathcal{S}_2, \quad (5.10)$$

as follows. The initial point of φ is one of our basepoints, lying along one of the walls, say w . Use the chosen normal vector on w to displace this point infinitesimally away from w . After this displacement the path φ may or may not cross w . If it does, we let $\mathcal{S}_1 = S_w^{-1}$, otherwise $\mathcal{S}_1 = 1$. Similarly the endpoint of φ lies along some w' . Displace it infinitesimally using the normal vector on w' . If after this displacement φ crosses w' , let $\mathcal{S}_2 = S_{w'}$, otherwise $\mathcal{S}_2 = 1$.

If the numbers \mathcal{D}_φ and S_w are chosen arbitrarily, there is no reason to expect that the $\rho(\varphi)$ satisfy the flatness constraints, corresponding to the homotopy relations in \mathcal{G}_C . As we did for $\mathcal{G}_{\Sigma'}$ above, we split these constraints into bulk constraints (for loops that do not go around branch points) and branch point constraints (for loops that do go around branch points on C). The fact that the matrices \mathcal{D}_φ obey the bulk constraints on Σ implies that they obey the bulk constraints on C as well. Moreover, in all examples we consider below (and more generally in all Fock-Goncharov or Fenchel-Nielsen networks), the branch point constraints on $\rho(\varphi)$ can be solved uniquely and determine the numbers S_w in terms of the \mathcal{D}_φ . Thus, for each choice of the \mathcal{D}_φ obeying the flatness constraints, we obtain a representation $\rho : \mathcal{G}_C \rightarrow SL(2)$ on C .

Suppose that we have two almost-flat equivariant representations $\rho^{\text{ab}}, \rho'^{\text{ab}}$ on Σ that are related by an equivalence g^{ab} . This implies that the corresponding sets of matrices $\mathcal{D}, \mathcal{D}'$ are related by the gauge transformation

$$g(z) = \begin{pmatrix} g(z^{(1)}) & 0 \\ 0 & g(z^{(2)}) \end{pmatrix}, \quad (5.11)$$

i.e. $\mathcal{D}'_\varphi = g(z_{i(\varphi)}) \mathcal{D}_\varphi g^{-1}(z_{f(\varphi)})$ for all paths φ on C . Then we obtain two $SL(2)$ representations ρ and ρ' on C , with unipotent matrices \mathcal{S}_w and \mathcal{S}'_w related by

$$\mathcal{S}'_w g(z_w) = g(z_w) \mathcal{S}_w. \quad (5.12)$$

The matrix g defines an equivalence between the $SL(2)$ representations ρ and ρ' , in the sense that g is a map $g : \mathcal{P}(C) \rightarrow SL(2)$ with

$$\rho'(\varphi) = g(z_{i(\varphi)}) \rho(\varphi) g(z_{f(\varphi)})^{-1}, \quad (5.13)$$

where for all boundary basepoints z_b we restrict $g(z_b) = 1$.

Hence, we have constructed a map

$$\Psi_{\mathcal{W}} : [\rho^{\text{ab}}] \mapsto [\rho] \quad (5.14)$$

which takes equivalence classes of almost-flat equivariant representations on Σ to equivalence classes of representations on C . This is the *nonabelianization map*.

Note that the representation ρ is precisely in the form to which we brought a \mathcal{W} -framed $SL(2)$ connection ∇ in §4: the parallel transports are diagonal within connected components of $C \setminus \mathcal{W}$, and the gauge transformation that relates adjacent components is unipotent.⁹ Moreover, the resulting representation ρ is \mathcal{W} -framed. Indeed, its monodromy matrix around a puncture z_i on C is of triangular shape, thus singling out an eigenline of the monodromy around z_i . Its monodromy around a boundary or interior component with the topology of an annulus is diagonal. Since the equivalences g do not interchange the two diagonal elements of this monodromy, we can choose a preferred eigenline for the monodromy in each direction. If we make this choice consistent with the discussion in §4.6, the nonabelianization map is the inverse of the abelianization map.

6 Examples

In this section we discuss a few instructive examples of the nonabelianization map. We emphasize the structure of the \mathcal{S} -matrices, the relation between the story for $SL(2)$ and $PSL(2)$, and the explicit identification of spectral coordinates with complex shear and complex length-twist coordinates.

6.1 Fock-Goncharov networks

First we describe the nonabelianization map for two examples of Fock-Goncharov networks, on the four-punctured sphere and on the one-punctured torus.

6.1.1 Four-punctured sphere

Consider the Fock-Goncharov network on the four-punctured sphere shown in Figure 4. We make a choice of basepoints $z_k \in \mathcal{P}_C$ and short paths $\wp_m \in \mathcal{G}_C$ as in Figure 31. Along each short path \wp_m we choose an $SL(2)$ matrix D_{\wp_m} that is diagonal if the path

⁹To make the relation between §4 and §5 more transparent, we could have introduced two basepoints z_w and z'_w along each wall w , infinitesimally displaced from the wall to either side. The gauge transformations acting on the bases $(s_1(z_w), s_2(z_w))$ and $(s'_1(z'_w), s'_2(z'_w))$, that are attached to the two sides of the wall w , correspond to the gauge transformations $g(z_w)$ and $g(z'_w)$. The branch point constraints do not have a solution for the *same* abelian representation ρ^{ab} unless $g(z_w) = g(z'_w)$. This corresponds to the statement that that the constraints on the bases $(s_1(z_w), s_2(z_w))$ and $(s'_1(z'_w), s'_2(z'_w))$ that bring the \mathcal{S} -matrices in unipotent form only leave a diagonal gauge transformation. The resulting configuration is equivalent to introducing just a single basepoint along every wall.

crosses a branch cut and strictly off-diagonal if it does not. For instance,

$$D_{\wp_1} = \begin{pmatrix} d_1 & 0 \\ 0 & d_1^{-1} \end{pmatrix}, \quad D_{\wp_6} = \begin{pmatrix} 0 & d_6 \\ -d_6^{-1} & 0 \end{pmatrix}. \quad (6.1)$$

The collection of matrices D_{\wp_m} forms an almost-flat equivariant abelian representation

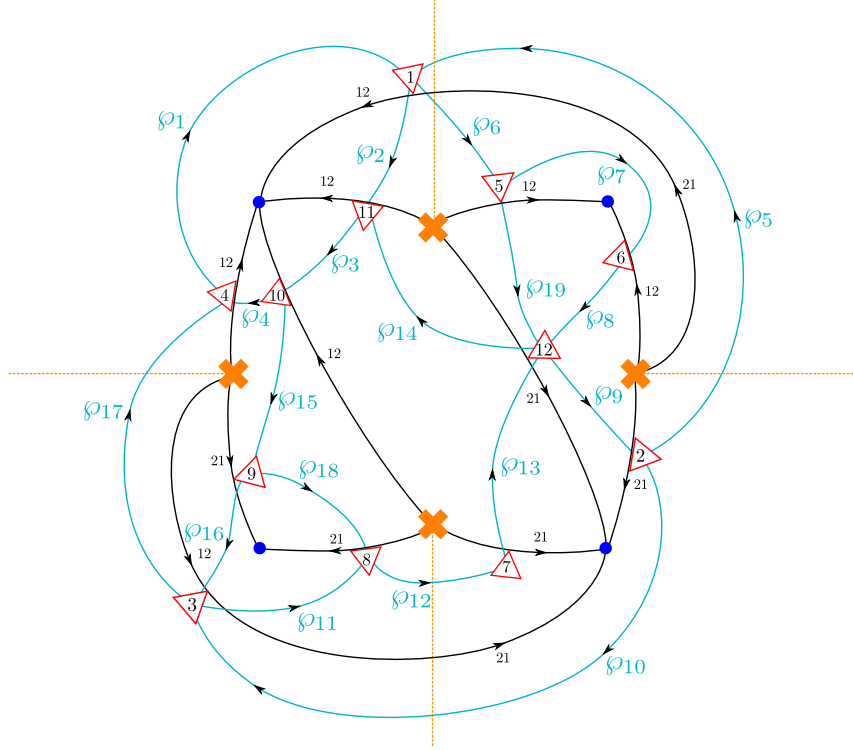


Figure 31: Spectral network on the four-punctured sphere with auxiliary data: blue lines are short paths; red arrows are basepoints; the direction of the red arrows specifies the normal vector at each wall.

ρ^{ab} if the matrices obey the bulk and branch point constraints. An example of a branch point constraint is

$$(D_{\wp_5} D_{\wp_6} D_{\wp_7} D_{\wp_8} D_{\wp_9})^2 = -\mathbf{1}. \quad (6.2)$$

(Trace out the corresponding loop in Figure 31 to see it encircles one branch point.) There are four such equations, which are automatically satisfied. Next let us consider the bulk equations. We choose abelian holonomies

$$M_{1,2}^{\text{ab}} = \begin{pmatrix} \mathcal{X}_{1,2}^{-1} & 0 \\ 0 & \mathcal{X}_{1,2} \end{pmatrix} \quad (6.3)$$

in the clockwise direction around the lifts of the punctures $z_{1,2}$ to the cover Σ , and similarly abelian holonomies

$$M_{3,4}^{\text{ab}} = \begin{pmatrix} \mathcal{X}_{3,4} & 0 \\ 0 & \mathcal{X}_{3,4}^{-1} \end{pmatrix} \quad (6.4)$$

in the clockwise direction around the lifts of the punctures $z_{3,4}$ to the cover. Then we enforce for instance

$$D_{\wp_1} D_{\wp_2} D_{\wp_3} D_{\wp_4} = M_1^{\text{ab}}. \quad (6.5)$$

There are four of these bulk equations, plus the equation at infinity

$$D_{\wp_1} D_{\wp_5}^{-1} D_{\wp_{10}} D_{\wp_{17}} = \mathbf{1}. \quad (6.6)$$

Thus the nineteen unknowns d_m are constrained by five equations in total, so that we have fourteen left-over degrees of freedom. This includes the gauge degrees of freedom, which we will discuss next.

Note that the short paths are oriented. The initial point of the path \wp_m is labeled by a number $i(m)$ and its final point by a number $f(m)$. Abelian gauge transformations act on the entries of the matrices D_{\wp_m} . When the matrix D_{\wp_m} is diagonal, with diagonal entries d_m and d_m^{-1} , a gauge transformation $g : \mathcal{P}_C \rightarrow \mathbb{C}$ acts as

$$d_m \rightarrow d_m \frac{g_{i(m)}}{g_{f(m)}}. \quad (6.7)$$

When D_{\wp_m} is strictly off-diagonal, it acts as

$$d_m \rightarrow d_m g_{i(m)} g_{f(m)}. \quad (6.8)$$

Fixing this abelian gauge freedom, i.e. choosing convenient values for the twelve g_k 's, only leaves two degrees of freedom in the d_k 's. These two unknowns correspond to gauge-invariant abelian holonomies around an A -cycle and B -cycle on the cover Σ . Let us name these abelian holonomies \mathcal{X}_A and \mathcal{X}_B . In this example we may choose

$$\mathcal{X}_A = d_2 d_{14}^{-1} d_9 d_5 \quad \text{and} \quad \mathcal{X}_B = d_5^{-1} d_{10} d_{16} d_{15} d_3 d_{14} d_8 d_7 d_6^{-1}. \quad (6.9)$$

Up to equivalence the abelian representation ρ^{ab} is determined completely in terms of the abelian holonomies $\mathcal{X}_A, \mathcal{X}_B, \mathcal{X}_1, \dots, \mathcal{X}_4$.

Having parameterized abelian almost-flat equivariant representations ρ^{ab} on the cover Σ we apply the non-abelianization map. We fix a normal vector at each basepoint z_k and write down a matrix \mathcal{S}_k as in equation (5.9). The matrix \mathcal{S}_k determines the transition function when crossing the wall in the direction of the normal vector. Whereas the abelian representation ρ^{ab} on a non-short path \wp , say $\wp = \wp_1 \wp_6$, with lift

$$\wp^{(12)} = \wp_1^{(11)} \wp_6^{(12)}, \quad (6.10)$$

is

$$\rho^{\text{ab}}(\wp^{(12)}) = \rho^{\text{ab}}(\wp_1^{(11)}) \rho^{\text{ab}}(\wp_6^{(12)}) = (D_{\wp_1} D_{\wp_6})_{12}, \quad (6.11)$$

the $SL(2)$ representation $\rho(\wp)$ is given by splicing in \mathcal{S} -matrices whenever the path \wp crosses a wall. In this example

$$\rho(\wp) = (D_{\wp_1} \mathcal{S}_1 D_{\wp_6}), \quad (6.12)$$

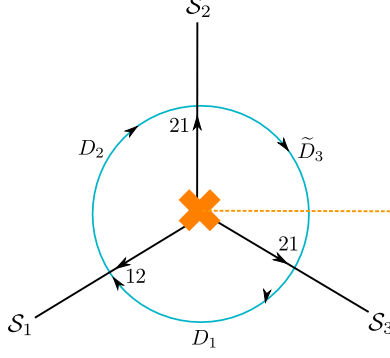


Figure 32: Local configuration around a branch point in a Fock-Goncharov network.

as can be read off from Figure 31. (We have inserted \mathcal{S}_1 instead of \mathcal{S}_1^{-1} since the red arrow labeled by 1 is oriented in the direction of the path \wp .)

Requiring the $SL(2)$ representation ρ to be flat is equivalent to enforcing non-abelian branch point constraints. There is one constraint for each branch point. For any branch point in a Fock-Goncharov network this constraint is of the form

$$D_1 \mathcal{S}_{1,ij} D_2 \mathcal{S}_{2,ji} \tilde{D}_3 \mathcal{S}_{3,ji} = \mathbf{1}, \quad (6.13)$$

where \tilde{D} is a strictly off-diagonal matrix. See Figure 32. The \mathcal{S} -wall matrices that appear in a branch point equation are fully determined by this constraint. Their off-diagonal elements are of the form

$$\mathcal{S}_{k,ij} = (D_{k+1} D_{k+2} D_{k+3})_{ij}^{-1}, \quad (6.14)$$

where one of the matrices D has a tilde on it. This element computes the abelian parallel transport along a path $a_k^{(ij)}$, that starts at the lift $z_k^{(i)}$ to the cover Σ , runs backwards along the wall w^{ij} until it hits a branch point, loops around the branch point, and follows the wall w^{ij} forwards to the lift $z_k^{(j)}$.

Now that we have determined the \mathcal{S} -matrices in terms of the abelian representation ρ^{ab} , we can give the complete $SL(2)$ representation ρ in terms of abelian data. In particular, we can compute the monodromies of ρ around any loop on C .

We fix a presentation of the fundamental group of C , i.e. four cycles $\mathcal{P}_1, \dots, \mathcal{P}_4$ with a common base point, chosen such that \mathcal{P}_p loops around the p th puncture, and with the relation $\mathcal{P}_1 \mathcal{P}_2 \mathcal{P}_3 \mathcal{P}_4 = 1$. Then we compute the $SL(2)$ monodromies $\mathcal{M}_{\mathcal{W}}(\mathcal{P}_p)$ in terms of the abelian data. For instance, if we choose

$$\mathcal{P}_1 = \wp_3 \wp_4 \wp_1 \wp_2 \quad (6.15)$$

the corresponding monodromy matrix is obtained by splicing in the \mathcal{S} -matrices,

$$\begin{aligned} M_{\mathcal{W}}(\mathcal{P}_1) &= D_{\wp_3} \mathcal{S}_{10} D_{\wp_4} \mathcal{S}_4 D_{\wp_1} \mathcal{S}_1 D_{\wp_2} \mathcal{S}_{11} \\ &= \begin{pmatrix} \mathcal{X}_1^{-1} & g \cdot \left(\mathcal{X}_1^{-1} + \frac{\mathcal{X}_2}{\mathcal{X}_1 \mathcal{X}_A} - \mathcal{X}_2 \mathcal{X}_B - \frac{\mathcal{X}_1 \mathcal{X}_2 \mathcal{X}_4 \mathcal{X}_A \mathcal{X}_B}{\mathcal{X}_3} \right) \\ 0 & \mathcal{X}_1 \end{pmatrix}, \end{aligned} \quad (6.16)$$

where g depends on our choice of gauge. After so doing we can check directly that

$$M_{\mathcal{W}}(\mathcal{P}_1) \cdot M_{\mathcal{W}}(\mathcal{P}_2) \cdot M_{\mathcal{W}}(\mathcal{P}_3) \cdot M_{\mathcal{W}}(\mathcal{P}_4) = 1, \quad (6.17)$$

and hence we have indeed constructed a family of \mathcal{W} -framed $SL(2)$ representations on the four-punctured sphere, in terms of the abelian holonomies $\mathcal{X}_A, \mathcal{X}_B$, as well as $\mathcal{X}_1, \dots, \mathcal{X}_4$.

Complexified shear coordinates

So far we have constructed \mathcal{W} -framed $SL(2)$ representations for Fock-Goncharov networks in terms of abelian data. Now let us discuss how the shear coordinates are explicitly realized in terms of the abelian data.

Recall the definition of the shear coordinates reviewed in §4.5, which assigns one shear coordinate to each edge of the ideal triangulation corresponding to the network. In our case this triangulation has six edges; we label the shear coordinates for these edges $\mathcal{Z}_1, \dots, \mathcal{Z}_6$ as illustrated in Figure 33. For instance,

$$\mathcal{Z}_2 = \frac{(s_1 \wedge s'_3)(s_2 \wedge s''_3)}{(s_2 \wedge s'_3)(s_1 \wedge s''_3)}. \quad (6.18)$$

Here s'_3 and s''_3 represent the parallel transport of the section s_3 along two inequivalent paths in the two triangles on either side of the edge labeled by the shear coordinate \mathcal{Z}_2 .

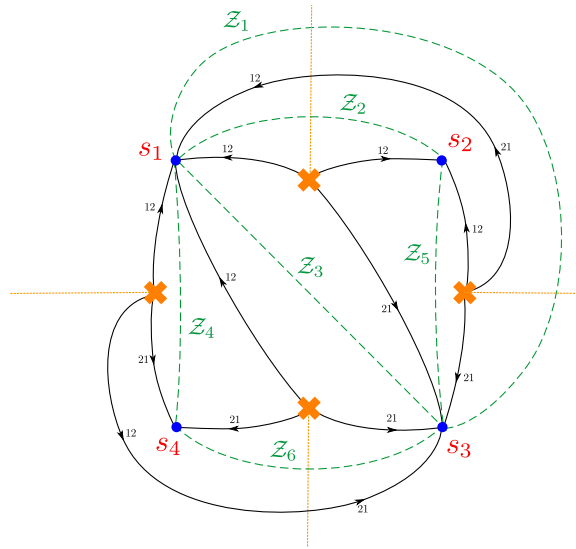


Figure 33: Ideal triangulation (in dark green) on the four-punctured sphere, and the corresponding shear coordinates $\mathcal{Z}_1, \dots, \mathcal{Z}_6$.

Now, from the discussion of §4.5 we expect that the shear coordinates \mathcal{Z}_E can be expressed in terms of abelian holonomies along odd cycles on Σ . Concretely, for example,

$$\mathcal{Z}_2 = (D_5 D_2 D_{14}^{-1} D_{19}^{-1} D_7 D_8 D_9)_{22}.$$

In turn these holonomies can be expressed in terms of $\mathcal{X}_A, \mathcal{X}_B, \mathcal{X}_1, \dots, \mathcal{X}_4$. Doing this we obtain

$$\begin{aligned} \mathcal{Z}_1 &= \mathcal{X}_1 \mathcal{X}_A \mathcal{X}_B, & \mathcal{Z}_2 &= -\frac{\mathcal{X}_2}{\mathcal{X}_A}, & \mathcal{Z}_3 &= \frac{\mathcal{X}_3}{\mathcal{X}_2 \mathcal{X}_4 \mathcal{X}_A \mathcal{X}_B}, \\ \mathcal{Z}_4 &= -\frac{\mathcal{X}_1 \mathcal{X}_4 \mathcal{X}_A}{\mathcal{X}_3}, & \mathcal{Z}_5 &= -\mathcal{X}_2 \mathcal{X}_A, & \mathcal{Z}_6 &= -\frac{\mathcal{X}_3 \mathcal{X}_4}{\mathcal{X}_1 \mathcal{X}_A}. \end{aligned} \quad (6.19)$$

As a check, the consecutive product of shear coordinates on the edges ending at the p th puncture should be equal to \mathcal{X}_p^2 .

If we attempt to invert the relations (6.19) to find the abelian holonomies (\mathcal{X} 's) in terms of the \mathcal{Z} 's, we find that the \mathcal{X} 's involve square roots in the \mathcal{Z} 's. This is consistent with the fact that the complex shear coordinates \mathcal{Z} do not completely determine a \mathcal{W} -framed $SL(2)$ representation, only its projection to $PSL(2)$. In contrast, the \mathcal{X} 's really do determine the full \mathcal{W} -framed $SL(2)$ representation.

Rather than comparing only the gauge invariant quantities (\mathcal{X} 's and \mathcal{Z} 's) we can also go a bit further and compare the actual $SL(2)$ parallel transport matrices which we obtain by nonabelianization (depending on \mathcal{X} 's) to the ones given in the Fock prescription (depending on \mathcal{Z} 's). This prescription was given in [23] (see also Appendix A of [3]). Let us briefly review it.

We compute the monodromy matrix $M_{\mathcal{F}}(\mathcal{P}_p)$ as follows. Follow the loop \mathcal{P}_p and write down a matrix

$$E(\mathcal{Z}_E) = \begin{pmatrix} 0 & \mathcal{Z}_E \\ 1 & 0 \end{pmatrix}, \quad (6.20)$$

when we cross an edge E labeled by the shear coordinates \mathcal{Z}_E . When turning right (left) inside a triangle, we write down the matrix V (V^{-1}) given by

$$V = \begin{pmatrix} -1 & -1 \\ 1 & 0 \end{pmatrix} \quad (6.21)$$

The monodromy matrix $M_{\mathcal{F}}(\mathcal{P}_p)$ is then the ordered product of the matrices $E(\mathcal{Z})$ and V , multiplied by a normalization factor which makes the determinant 1. For example, in our case

$$M_{\mathcal{F}}(\mathcal{P}_1) = \pm \mathcal{X}_1^{-1} E(\mathcal{Z}_3) V E(\mathcal{Z}_4) V E(\mathcal{Z}_1) V E(\mathcal{Z}_2) V. \quad (6.22)$$

The normalization factor is only determined up to a sign, so the resulting $M_{\mathcal{F}}(\mathcal{P})$ is really valued in $PSL(2)$. We want to compare the $M_{\mathcal{F}}(\mathcal{P})$ with the matrices $M_{\mathcal{W}}(\mathcal{P}_p)$ which arise from nonabelianization, which are really $SL(2)$ -valued. Thus we fix the sign in $M_{\mathcal{F}}(\mathcal{P})$ in such a way that the eigenvalues match: denote the resulting $SL(2)$ -valued matrices by $M_{\mathcal{F}}^s(\mathcal{P}_p)$. After so doing, we can indeed verify directly that the monodromy matrices $M_{\mathcal{F}}^s(\mathcal{P}_p)$ and $M_{\mathcal{W}}(\mathcal{P}_p)$ are conjugate.

This comparison also gives a concrete way of seeing how the reduction from $SL(2)$ representations to $PSL(2)$ representations works on the level of the spectral coordinates. Let us call the $SL(2)$ representation ρ , as before, and its reduction to a $PSL(2)$ representation $\tilde{\rho}$. The normalization factors of the Fock matrices $M_{\mathcal{F}}(\mathcal{P}_{1,2,3,4})$ are given by $1/\mathcal{X}_1$,

\mathcal{X}_2 , $\mathcal{X}_1/(\mathcal{X}_2\mathcal{X}_4)$ and \mathcal{X}_4 , respectively, and are dependent on the choice of the lift of $\tilde{\rho}$ to ρ . In contrast, the shear coordinates Z_E should only depend on $\tilde{\rho}$. This suggests that lifts of $\tilde{\rho}$ to $SL(2)$ are related to one another by

$$\begin{aligned}\mathcal{X}_1 &\rightarrow s_1 \mathcal{X}_1 \\ \mathcal{X}_2 &\rightarrow s_2 \mathcal{X}_2 \\ \mathcal{X}_4 &\rightarrow s_3 \mathcal{X}_4,\end{aligned}\tag{6.23}$$

where $s_1, s_2, s_3 \in \{\pm 1\}$. Indeed, from the relations (6.19) it is easy to see that this operation can be uniquely completed to a transformation on all the abelian holonomies $\mathcal{X}_A, \mathcal{X}_B, \mathcal{X}_1, \dots, \mathcal{X}_4$, in such a way that the shear coordinates Z_E stay invariant. Thus, if we form equivalence classes of abelian representations that are related by the (completed) sign mapping s , we find a one-to-one map to $PSL(2)$ representations.

6.1.2 Once-punctured torus

Next, we work out the nonabelianization map for a Fock-Goncharov network on the once-punctured torus. Figure 34 illustrated the spectral network together with a choice of basepoints and short paths \wp .

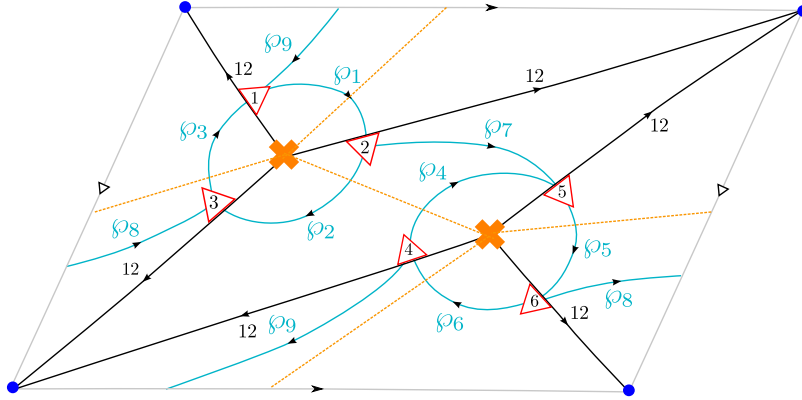


Figure 34: Spectral network on the once-punctured torus with auxiliary data.

We choose an $SL(2)$ matrix D_\wp along each short path \wp that is diagonal if the path crosses a branch-cut and strictly off-diagonal if it does not. In this example these matrices have 9 degrees of freedom d_\wp . The collection of matrices D_\wp forms an almost-flat equivariant abelian representation ρ^{ab} if the matrices obey the branch point and bulk constraints.

The branch point constraints enforce that the abelian holonomy around a branch point equals minus the identity, i.e. such that the abelian representation is “almost flat”. There are two such equations in this example, which are automatically satisfied.

There are three bulk equations that fix the abelian holonomies around lifts of the three

1-cycles on the once-punctured torus to the cover. They read

$$\begin{aligned} M_a^{\text{ab}} &= D_9 D_1 D_7 D_4^{-1}, \\ M_b^{\text{ab}} &= D_8 D_2^{-1} D_7 D_5, \\ M_m^{\text{ab}} &= D_8 D_3 D_9^{-1} D_4 D_7^{-1} D_2 D_8^{-1} D_6 D_9 D_1 D_7 D_5, \end{aligned} \quad (6.24)$$

where we define

$$M_{a,b,m}^{\text{ab}} = \begin{pmatrix} \mathcal{X}_{a,b,m} & 0 \\ 0 & \mathcal{X}_{a,b,m}^{-1} \end{pmatrix}. \quad (6.25)$$

Up to gauge degrees of freedom this completely fixes the almost-flat equivariant abelian representation in terms of the abelian holonomies \mathcal{X}_a , \mathcal{X}_b and \mathcal{X}_m .

The next step is to apply the nonabelianization map. We determine the \mathcal{S} -matrices using the non-abelian branch point equations, exactly as in the previous example, and find the resulting $SL(2)$ representation ρ in terms of abelian data.

Having fixed a presentation of the fundamental group of the once-punctured torus, i.e. three cycles \mathcal{P}_a , \mathcal{P}_b and \mathcal{P}_m with the relation

$$\mathcal{P}_a \mathcal{P}_b \mathcal{P}_a^{-1} \mathcal{P}_b^{-1} = \mathcal{P}_m, \quad (6.26)$$

we compute the $SL(2)$ monodromy matrices $M_{\mathcal{W}}(\mathcal{P}_{a,b,m})$ around these cycles, and verify that indeed

$$M_{\mathcal{W}}(\mathcal{P}_a) M_{\mathcal{W}}(\mathcal{P}_b) M_{\mathcal{W}}(\mathcal{P}_a)^{-1} M_{\mathcal{W}}(\mathcal{P}_b)^{-1} = M_{\mathcal{W}}(\mathcal{P}_m). \quad (6.27)$$

For instance,

$$\begin{aligned} M_{\mathcal{W}}(\mathcal{P}_a) &= D_7 D_4^{-1} \mathcal{S}_4^{-1} D_9 D_1 \mathcal{S}_2 \\ &= \begin{pmatrix} \mathcal{X}_a^{-1} & \\ \mathcal{X}_a \mathcal{X}_b^2 \mathcal{X}_m^{-1} g^{-1} & \mathcal{X}_a (\mathcal{X}_b^2 + \mathcal{X}_m) \mathcal{X}_m^{-1} \end{pmatrix}, \end{aligned} \quad (6.28)$$

where g is a gauge-dependent quantity.

As in the previous example, we want to compare these monodromy matrices with those which arise from the Fock prescription. In this example there are three shear coordinates $\mathcal{Z}_{1,2,3}$. Expressed in terms of the abelian holonomies $\mathcal{X}_{a,b,m}$ they read

$$\mathcal{Z}_1 = \mathcal{X}_a^2 \mathcal{X}_m^{-1} \quad \mathcal{Z}_2 = \mathcal{X}_b^2 \mathcal{X}_m^{-1} \quad \mathcal{Z}_3 = \mathcal{X}_m \mathcal{X}_a^{-2} \mathcal{X}_b^{-2}. \quad (6.29)$$

Notice that even though \mathcal{X}_m can be expressed as a ratio of shear coordinates, \mathcal{X}_a and \mathcal{X}_b cannot.

We compute the Fock matrices $M_{\mathcal{F}}^{\mathcal{S}}(\mathcal{P}_{a,b,m})$ as

$$\begin{aligned} M_{\mathcal{F}}^+(\mathcal{P}_a) &= \mathcal{X}_a E(\mathcal{Z}_3) V E(\mathcal{Z}_2) V^{-1} \\ M_{\mathcal{F}}^+(\mathcal{P}_b) &= \mathcal{X}_b E(\mathcal{Z}_3) V^{-1} E(\mathcal{Z}_1) V \\ M_{\mathcal{F}}^+(\mathcal{P}_b) &= M_{\mathcal{F}}^+(\mathcal{P}_a) M_{\mathcal{F}}^+(\mathcal{P}_b) M_{\mathcal{F}}^+(\mathcal{P}_a)^{-1} M_{\mathcal{F}}^+(\mathcal{P}_b)^{-1}, \end{aligned}$$

and compare them to the spectral matrices $M_{\mathcal{W}}(\mathcal{P}_{a,b,m})$. As before, we find that the two sets of matrices are conjugate.

To understand how the reduction from $SL(2)$ to $PSL(2)$ representations acts on the abelian representations, we consider the transformation

$$\begin{aligned}\mathcal{X}_a &\rightarrow s_a \mathcal{X}_a \\ \mathcal{X}_b &\rightarrow s_b \mathcal{X}_a \\ \mathcal{X}_m &\rightarrow \mathcal{X}_m,\end{aligned}\tag{6.30}$$

with $s_a, s_b \in \{\pm 1\}$. Clearly this leaves the shear coordinates \mathcal{Z}_E invariant (and hence leaves the $PSL(2)$ representation invariant), while changing the $SL(2)$ representation ρ . Thus, if we form equivalence classes of abelian representations that are related by the sign mapping s , we find that they are in one-to-one correspondence with $PSL(2)$ representations.

6.2 Fenchel-Nielsen examples

Next we study the nonabelianization map for Fenchel-Nielsen networks. We apply the nonabelianization map to molecule I and II on the three-holed sphere, and to Fenchel-Nielsen networks on the four-holed sphere and the genus two surface. We explicitly relate the spectral coordinates to a complexified version of length and twist coordinates.

6.2.1 Pair of pants: molecule I

We start with the spectral network “molecule I” on the three-holed sphere. As always, we begin by fixing the auxiliary data. We fix a basepoint $z_{a,b,c}$ for each double wall and short paths \wp in between the basepoints. Additionally, we fix a basepoint $z_{1,2,3}$ on each boundary component and choose a + direction on it. All choices are illustrated in Figure 35.

As before, we choose an $SL(2)$ matrix D_\wp along each short path \wp that is diagonal if the path crosses a branch-cut and strictly off-diagonal if it does not. In this example these matrices have 9 degrees of freedom d_\wp . The collection of matrices D_\wp forms an almost-flat equivariant abelian representation ρ^{ab} if the matrices obey the branch point and bulk constraints.

The branch point constraints enforce that the abelian holonomy around a branch point equals minus the identity, *i.e.* such that the abelian representation is “almost flat”. There are two such equations in this example, which are automatically satisfied. The bulk equations fix the boundary conditions. We choose a closed path $\gamma_{1,2,3}$ along each boundary component (in the + direction attached to the boundary component), and enforce the abelian holonomy along the lift $\gamma_{1,2,3}^{(ii)}$ to be equal to the i th diagonal entry of the matrix¹⁰

$$M_{1,2,3}^{\text{ab}} = \begin{pmatrix} \mathcal{X}_{1,2,3} & 0 \\ 0 & \mathcal{X}_{1,2,3}^{-1} \end{pmatrix},\tag{6.31}$$

¹⁰This condition is consistent with the discussion in §4.6, since the + direction on the boundary components coincides with the orientation of the 21 walls.

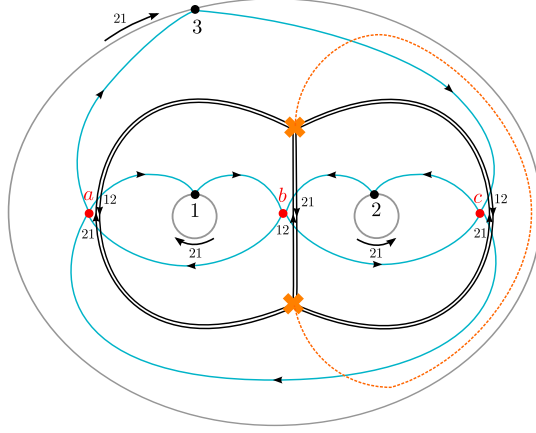


Figure 35: Molecule I with a marked point on each boundary (black dot), a basepoint close to each double wall (red dot) and a collection of short paths (blue lines). The boundary components are labeled as 1, 2 and 3 (in black) and the double walls as a , b and c (in red). The arrow on each boundary component indicates the + orientation.

where $\mathcal{X}_{1,2,3} \neq 0, \pm 1$.¹¹

These are three constraints on the nine unknowns d_φ . Gauge transformations at the marked points $z_{a,b,c}$ reduce the number of unknowns to three. The three remaining unknowns can be expressed in terms of abelian holonomies $\mathcal{X}_{12,23,31}$ along open paths that run from one boundary component to another. We can choose to additionally divide out by constant gauge transformations at the boundary marked points $z_{1,2,3}$, in which case the number of unknowns reduces to zero.

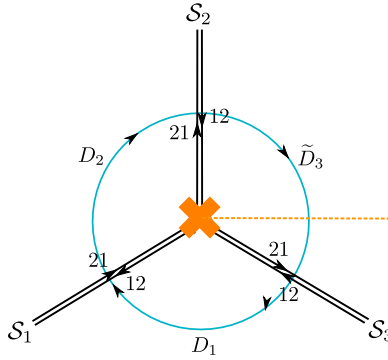


Figure 36: Local configuration around a branch point in a Fenchel-Nielsen network.

Having parametrized abelian almost-flat equivariant representations ρ_{ab} on the cover Σ we find the non-abelianization map. We construct a nonabelian representation $\rho(\varphi)$ by splicing in \mathcal{S} -matrices whenever the path φ crosses a wall. Requiring the non-abelian

¹¹To restrict to irreducible representations we furthermore impose that $\mathcal{X}_1 \neq \mathcal{X}_2\mathcal{X}_3$, $\mathcal{X}_2 \neq \mathcal{X}_3\mathcal{X}_1$, $\mathcal{X}_3 \neq \mathcal{X}_1\mathcal{X}_2$ and $\mathcal{X}_1\mathcal{X}_2\mathcal{X}_3 \neq 1$. We find that these constraints translate to the constraints that we imposed when abelianizing Fenchel-Nielsen networks at the level of the image of the non-abelianization map (see for instance Proposition 3.2 in [24]).

representation ρ to be flat is equivalent to enforcing non-abelian branch point constraints. There is one constraint for each branch point. For any branch point in a Fenchel-Nielsen network this constraint is of the form

$$D_1 \mathcal{S}_{1,12}^{\text{out}} \mathcal{S}_{1,21}^{\text{in}} D_2 \mathcal{S}_{2,21}^{\text{out}} \mathcal{S}_{2,12}^{\text{in}} \tilde{D}_3 \mathcal{S}_{3,21}^{\text{out}} \mathcal{S}_{3,12}^{\text{in}} = \mathbf{1}, \quad (6.32)$$

where \tilde{D} is a strictly off-diagonal matrix. See Figure 36. The \mathcal{S} -wall matrices that appear in this branch point equation are partly determined by this equation. Their off-diagonal elements are of the form

$$\begin{aligned} \mathcal{S}_{1,12}^{\text{out}} &= \mathcal{X}(a_1^{(12)}) f_1 & \mathcal{S}_{1,21}^{\text{in}} &= \mathcal{X}(a_1^{(12)})^{-1} (f_2 - 1) \\ \mathcal{S}_{2,21}^{\text{out}} &= \mathcal{X}(a_2^{(21)}) f_2 & \mathcal{S}_{2,12}^{\text{in}} &= \mathcal{X}(a_2^{(21)})^{-1} (f_3 - 1) \\ \mathcal{S}_{3,21}^{\text{out}} &= \mathcal{X}(a_3^{(21)}) f_3 & \mathcal{S}_{3,12}^{\text{in}} &= \mathcal{X}(a_3^{(21)})^{-1} (f_1 - 1), \end{aligned} \quad (6.33)$$

where the factors f_k are arbitrary, and $\mathcal{X}(a_k^{(ij)})$ are abelian holonomies along the auxiliary paths

$$a_k^{(ij)} = (\wp_{k+1} \wp_{k+2} \wp_{k+3})_{(ij)}^{-1}.$$

We already encountered these auxiliary factors in the Fock-Goncharov examples. The additional factors f_k are new to Fenchel-Nielsen type networks.

All \mathcal{S} -matrices are fully determined once we impose the nonabelian branch point equations for every branch point in the spectral network. For instance, consider the \mathcal{S} -matrix attached to the double wall (w_a^{21}, w_a^{12}) on the left in Figure 35. When crossing the double wall from the left to the right, this matrix can be written in the form

$$\mathcal{S}_a = \begin{pmatrix} 1 & 0 \\ \mathcal{S}(w_a^{21}) & 1 \end{pmatrix} \begin{pmatrix} 1 & \mathcal{S}(w_a^{12}) \\ 0 & 1 \end{pmatrix}, \quad (6.34)$$

with off-diagonal components

$$\mathcal{S}(w_a^{12}) = \mathcal{X}(a_a^{12}) \left(\frac{1 + \mathcal{X}_b^2}{1 - \mathcal{X}_a^2 \mathcal{X}_b^2} \right) \quad (6.35)$$

$$\mathcal{S}(w_a^{21}) = \mathcal{X}(a_a^{21}) \left(\frac{1 + \mathcal{X}_c^2}{1 - \mathcal{X}_a^2 \mathcal{X}_c^2} \right), \quad (6.36)$$

where we redefined $\mathcal{X}_1 = \mathcal{X}_a \mathcal{X}_b$, $\mathcal{X}_2 = \mathcal{X}_b \mathcal{X}_c$ and $\mathcal{X}_3 = \mathcal{X}_a \mathcal{X}_c$. The novel factor in these \mathcal{S} -matrices is an infinite sum of monomials in the coordinates $\mathcal{X}_{a,b,c}$.

The interpretation for each monomial in the sum is best understood from the limiting spectral network illustrated in Figure 37. The term

$$\mathcal{X}(a_a^{12})$$

computes the abelian parallel transport along a path on Σ that starts at the red dot labeled by 1 (lifted to the first sheet of the cover), follows the (black part of the) orange wall to

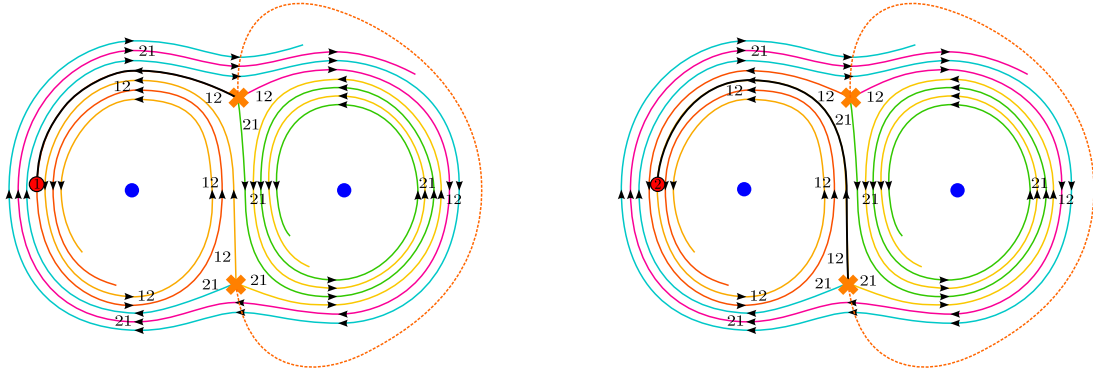


Figure 37: Left and right illustrate the interpretation of the terms $\mathcal{X}(a_a^{12})$ and $\mathcal{X}(a_a^{12})\mathcal{X}_b^2$ in the \mathcal{S} -matrices, respectively, in the limiting spectral network to molecule II.

the upper branch point, circles around it, and runs back to the same red dot (lifted to the second sheet of the cover). The term

$$\mathcal{X}(a_a^{12}) \mathcal{X}_b^2$$

computes the abelian parallel transport along a path that starts at the red dot labeled by 2 (lifted to the first sheet of the cover), follows the (black part of the) yellow wall all the way to the lower branch point, circles around it, and runs back to the same red dot (lifted to the second sheet of the cover). All other monomials in the \mathcal{S} -wall matrices can be explained similarly.

The \mathcal{S} -matrices attached to the two other double walls in the spectral network are related to \mathcal{S}_a using the cyclic symmetry of the spectral network.

Length-twist coordinates

The resulting \mathcal{W} -framed $SL(2)$ representation ρ has a diagonal monodromy matrix

$$\rho(\gamma_{1,2,3}) = \begin{pmatrix} \mathcal{X}_{1,2,3} & 0 \\ 0 & \mathcal{X}_{1,2,3}^{-1} \end{pmatrix} \quad (6.37)$$

along the closed paths $\gamma_{1,2,3}$ that follow the boundary component in the + direction. The abelian holonomies $\mathcal{X}_{1,2,3}$ are each equal to a square-root of an exponentiated complex Fenchel-Nielsen length parameter. Thus we have found that these length parameters occur as an example of spectral parameters.

Since we fixed a trivialization at the boundary marked points, the \mathcal{W} -framed representation ρ not only depends on the abelian holonomies $\mathcal{X}_{1,2,3}$, but also on the abelian holonomies $\mathcal{X}_{12,23,31}$ along open paths that begin and end on different boundary components. If we divide out by constant gauge transformations at the marked points, we find a representation that is unique (up to gauge equivalence) once we fix the eigenvalues $\mathcal{X}_{1,2,3}$.

We can furthermore reduce to \mathcal{W} -framed $PSL(2)$ representations by identifying almost-flat equivariant representations that are related by the action of $H^1(C, \mathbb{Z}/2\mathbb{Z})$ given by

$$(\mathcal{X}_1, \mathcal{X}_2, \mathcal{X}_3) \mapsto (\epsilon_1 \mathcal{X}_1, \epsilon_2 \mathcal{X}_2, \epsilon_3 \mathcal{X}_3), \quad (6.38)$$

parametrized by the triple $(\epsilon_1, \epsilon_2, \epsilon_3) \in (\mathbb{Z}/2\mathbb{Z})^3$ satisfying $\epsilon_1 \epsilon_2 \epsilon_3 = 1$ (see also [24]).

6.2.2 Pair of pants: molecule II

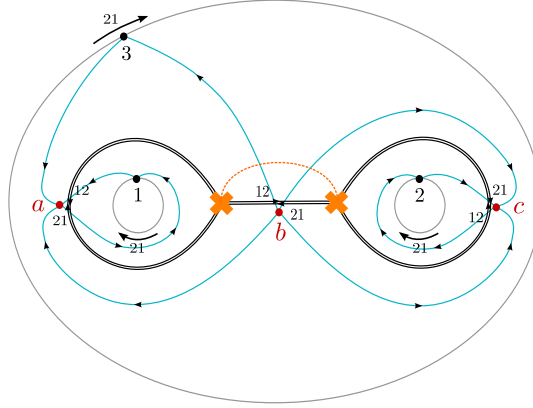


Figure 38: Molecule II with a marked point on each boundary (black dot), a basepoint close to each double wall (red dot) and a collection of short paths (blue lines). The boundary components are labeled as 1, 2 and 3 (in black) and the double walls as a , b and c (in red). The arrow on each boundary component indicates the + orientation

The description of the nonabelianization map for molecule II is similar to that for molecule I. We can for instance determine it using the data in Figure 38. The off-diagonal components of the \mathcal{S} -matrices are functions of the abelian holonomies $\mathcal{X}_{1,2,3}$ along closed paths $\gamma_{1,2,3}$ homotopic to the respective boundary components. If we redefine these parameters through the equations $\mathcal{X}_1 = \mathcal{X}_a$, $\mathcal{X}_2 = \mathcal{X}_c$ and $\mathcal{X}_3 = 1/(\mathcal{X}_a \mathcal{X}_b^2 \mathcal{X}_c)$, the off-diagonal components are power series in the parameters $\mathcal{X}_{a,b,c}$. Crossing the 21-wall first and the 12-wall last, we have

$$\mathcal{S}_{a,b,c} = \begin{pmatrix} 1 & 0 \\ \mathcal{S}(w_{a,b,c}^{21}) & 1 \end{pmatrix} \begin{pmatrix} 1 & \mathcal{S}(w_{a,b,c}^{12}) \\ 0 & 1 \end{pmatrix}, \quad (6.39)$$

where

$$\begin{aligned} \mathcal{S}(w_a^{12}) &= \mathcal{X}(a_a^{12}) \frac{1}{(1-\mathcal{X}_a^2)} & \mathcal{S}(w_a^{21}) &= \mathcal{X}(a_a^{21}) \frac{(1+\mathcal{X}_b^2)(1+\mathcal{X}_c^2 \mathcal{X}_b^2)}{1-\mathcal{X}_a^2 \mathcal{X}_b^4 \mathcal{X}_c^2} \\ \mathcal{S}(w_b^{12}) &= \mathcal{X}(a_b^{12}) \frac{1+\mathcal{X}_a^2(1+(1+\mathcal{X}_c^2)\mathcal{X}_b^2)}{1-\mathcal{X}_a^2 \mathcal{X}_b^4 \mathcal{X}_c^2} & \mathcal{S}(w_b^{21}) &= \mathcal{X}(a_b^{21}) \frac{1+\mathcal{X}_c^2(1+(1+\mathcal{X}_a^2)\mathcal{X}_b^2)}{1-\mathcal{X}_a^2 \mathcal{X}_b^4 \mathcal{X}_c^2} \\ \mathcal{S}(w_c^{12}) &= \mathcal{X}(a_c^{12}) \frac{1}{(1-\mathcal{X}_c^2)} & \mathcal{S}(w_c^{21}) &= \mathcal{X}(a_c^{21}) \frac{(1+\mathcal{X}_b^2)(1+\mathcal{X}_a^2 \mathcal{X}_b^2)}{(1-\mathcal{X}_a^2 \mathcal{X}_b^4 \mathcal{X}_c^2)}. \end{aligned} \quad (6.40)$$

As the reader can verify, all monomials in the \mathcal{S} -matrices can be interpreted as abelian holonomies along auxiliary paths in the limiting network (which is illustrated in Figure 10).

6.2.3 Four-holed sphere

Given a pair of pants decomposition of the four-holed sphere, we can build a Fenchel-Nielsen type spectral network choosing either molecule I or II on each pair of pants. Let us for instance determine the nonabelianization map for the spectral network illustrated in Figure 39, *i.e.* a union of two molecules of type II.

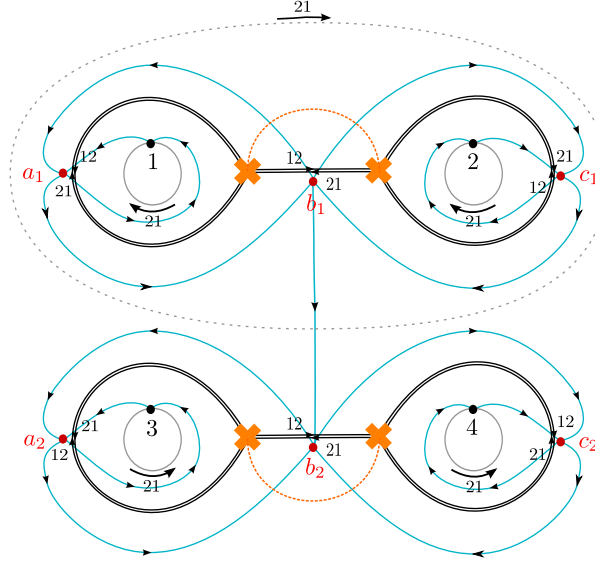


Figure 39: Maximally degenerate spectral network on the four-holed sphere with a basepoint on each boundary (black dot), a basepoint for each wall (red dot) and a collection of short paths (blue lines). Additionally, an arrow denotes the + direction on every boundary component and on the curve that defines the pants decomposition.

We fix four basepoints $z_{1,2,3,4}$ on the boundary components, six basepoints $z_{a_{1,2}, b_{1,2}, c_{1,2}}$ on the double walls and we choose 13 short paths φ , as is illustrated in Figure 39. In total, the matrices D_φ thus contain 13 variables. The bulk constraints consist of boundary conditions at the boundaries and at infinity, and reduce the number of variables to 8. After fixing the 6 gauge degrees of freedom (one at each basepoint at a double wall), we are left with two gauge-invariant abelian holonomies. Let us call these spectral coordinates \mathcal{X}_A and \mathcal{X}_B .

The cover Σ of the 4-holed sphere is an 8-holed torus. The abelian holonomies $\mathcal{X}_{1,2,3,4}^\pm$ along the boundary components are part of the boundary conditions that we have just imposed.¹² The coordinates \mathcal{X}_A and \mathcal{X}_B are abelian holonomies along a choice of paths A and B on the cover Σ that intersect each other once. To be explicit, let the path A be a lift to sheet 1 of Σ of the path α that defines the pants decomposition (see Figure 40). We take B as the lift of a path β in Figure 40, lifted and oriented in such a way that $A\#B = 1$.¹³

¹²Consistent with choices in §4.6, we enforce the abelian holonomy around sheet 1 to be $\mathcal{X}_{1,2,3,4}$.

¹³We furthermore impose the constraints that $\mathcal{X}_{1,2,3,4,A} \neq 0, \pm 1$, and that when restricted to each pair of pants $\mathcal{X}_{i_1} \neq \mathcal{X}_{i_2} \mathcal{X}_{i_3}$, $\mathcal{X}_{i_2} \neq \mathcal{X}_{i_3} \mathcal{X}_{i_1}$, $\mathcal{X}_{i_3} \neq \mathcal{X}_{i_1} \mathcal{X}_{i_2}$ and $\mathcal{X}_{i_1} \mathcal{X}_{i_2} \mathcal{X}_{i_3} \neq 1$. These constraints are equivalent to the constraints that we imposed when abelianizing with Fenchel-Nielsen networks [24].

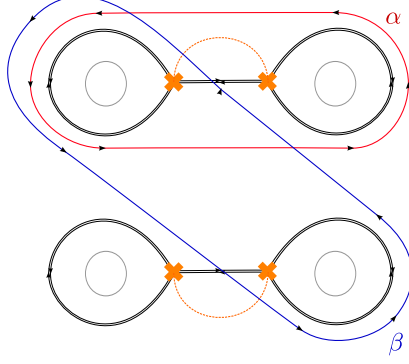


Figure 40: Choice of paths α and β on the four-holed sphere.

Having parametrized abelian almost-flat equivariant representations ρ_{ab} on the cover Σ , we construct the nonabelian representations ρ on the four-holed sphere by splicing in \mathcal{S} -matrices. These \mathcal{S} -matrices are completely determined by the non-abelian branch point equations. As can be expected, we find that the \mathcal{S} -matrices are similar to those for the molecule II network on the three-holed sphere.

More precisely, the off-diagonal components of the \mathcal{S} -matrices for the top (bottom) molecule are equal to those in equation (6.40) if we apply a change of variables

$$(\mathcal{X}_a, \mathcal{X}_b, \mathcal{X}_c) \mapsto (\mathcal{X}_{a_1}, \mathcal{X}_{b_1}, \mathcal{X}_{c_1})$$

(or $(\mathcal{X}_a, \mathcal{X}_b, \mathcal{X}_c) \mapsto (\mathcal{X}_{a_2}, \mathcal{X}_{b_2}, \mathcal{X}_{c_2})$). These variables are defined in such a way that $\mathcal{X}_1 = \mathcal{X}_{a_1}, \mathcal{X}_2 = \mathcal{X}_{c_1}, \mathcal{X}_3 = \mathcal{X}_{a_2}, \mathcal{X}_4 = \mathcal{X}_{c_2}$ are the abelian holonomies around loops $\mathcal{P}_{1,2,3,4}^{(11)}$ that go around the boundary components in the + direction. Furthermore,

$$\mathcal{X}_A = 1/(\mathcal{X}_{a_1} \mathcal{X}_{b_1}^2 \mathcal{X}_{c_1}) = 1/(\mathcal{X}_{a_2} \mathcal{X}_{b_2}^2 \mathcal{X}_{c_2})$$

is the abelian holonomy along the path A .

The given parametrization of the almost-flat equivariant abelian representations ρ^{ab} , together with the equations for the \mathcal{S} -matrices, determine the nonabelianization map explicitly. Monodromy matrices of the resulting $SL(2)$ representations ρ can be expressed purely in terms of abelian data: the four given abelian holonomies $\mathcal{X}_{1,2,3,4}$ along paths around the boundary components, the abelian holonomies along open paths that run from one boundary component to another and the abelian holonomies \mathcal{X}_A and \mathcal{X}_B around path A and B . If we divide out the constant gauge transformations at the boundary marked points, the image of the nonabelianization map is a two-parameter family of \mathcal{W} -framed $SL(2)$ representations $[\rho(\mathcal{X}_A, \mathcal{X}_B)]$.

Length-twist coordinates

The $SL(2)$ monodromy matrices around the paths α and $\mathcal{P}_{1,2,3,4}$ are all diagonal, of the form

$$\rho(\alpha, \mathcal{P}_{1,2,3,4}) = \begin{pmatrix} \mathcal{X}_{A,1,2,3,4} & 0 \\ 0 & \mathcal{X}_{A,1,2,3,4}^{-1} \end{pmatrix}. \quad (6.41)$$

The abelian holonomies $\mathcal{X}_{1,2,3,4,A}$ are equal to square-roots of the exponentiated, complexified Fenchel-Nielsen length parameters.

In particular, we have found that the spectral coordinate \mathcal{X}_A is the square-root of the exponentiated, complexified Fenchel-Nielsen length coordinate. Much less trivial from this construction is that the spectral coordinate \mathcal{X}_B is the exponential of a complexified Fenchel-Nielsen twist parameter.

We verify this claim by comparing the traces of the monodromy matrices for ρ with a complex version of Okai's formula, which computes these traces in terms of the Fenchel-Nielsen twist parameter [25]. (We also found it helpful to look at Kabaya's analysis in [24], in which a set of matrix generators of $SL(2, \mathbb{C})$ flat connections is systematically found in terms of a complexified version of the Fenchel-Nielsen coordinates and compared to Okai's formula for Fuchsian representations.)

Let us focus on the monodromy matrix M_β along the path β , illustrated in Figure 40. On the one hand, Okai's formula computes the trace of this monodromy as

$$\text{Tr } M_\beta = \sqrt{c} \left(\frac{t}{\mathcal{X}_A} + \frac{\mathcal{X}_A}{t} \right) + d, \quad (6.42)$$

in terms of the Fenchel-Nielsen twist parameter t . The coefficients c and d are given by

$$c = \frac{1}{(\mathcal{X}_A - \mathcal{X}_A^{-1})^4} \left(\mathcal{Z}_A^2 + \mathcal{Z}_1^2 + \mathcal{Z}_2^2 - \mathcal{Z}_A \mathcal{Z}_1 \mathcal{Z}_2 - 4 \right) \left(\mathcal{Z}_A^2 + \mathcal{Z}_3^2 + \mathcal{Z}_4^2 - \mathcal{Z}_A \mathcal{Z}_3 \mathcal{Z}_4 - 4 \right)$$

$$d = \frac{1}{(\mathcal{X}_A - \mathcal{X}_A^{-1})^2} \left(\mathcal{Z}_A (\mathcal{Z}_2 \mathcal{Z}_4 + \mathcal{Z}_1 \mathcal{Z}_3) - 2(\mathcal{Z}_1 \mathcal{Z}_4 + \mathcal{Z}_2 \mathcal{Z}_3) \right),$$

and $\mathcal{Z}_A = \mathcal{X}_A + \mathcal{X}_A^{-1}$ and $\mathcal{Z}_p = \mathcal{X}_p + \mathcal{X}_p^{-1}$. On the other hand, the trace of the monodromy matrix M_β for the nonabelianized representation ρ is given by

$$\text{Tr } M_\beta = - \left(\mathcal{X}_B + \frac{c}{\mathcal{X}_B} \right) + d. \quad (6.43)$$

Comparing the two formulas we conclude that

$$t = - \left(\frac{\mathcal{X}_A}{\sqrt{c}} \right) \mathcal{X}_B. \quad (6.44)$$

In other words, the spectral coordinate \mathcal{X}_B is the exponential of a complexified version of a Fenchel-Nielsen twist coordinate.

Even though the precise form of the multiplicative factor depends on characteristics of the chosen Fenchel-Nielsen network, we find that the spectral coordinate \mathcal{X}_B is always proportional to the Fenchel-Nielsen parameter t .

Of course, in this comparison we have to be careful to match the $SL(2)$ monodromies around the same 1-cycle β . If we compute the $SL(2)$ monodromy along any other choice of 1-cycle β' that intersects the 1-cycle α once, equation (6.43) holds in a modified form

$$\text{Tr } M_{\beta'} = - \left(\mathcal{X}_{B'} + \frac{c'}{\mathcal{X}_{B'}} \right) + d', \quad (6.45)$$

where B' is a lift of β' to the covering (following the same rules as before). For any such choice we find that the abelian holonomy $\mathcal{X}_{B'}$ is a twist coordinate (by comparing to formulae in [25, 24]).

We can reduce to $PSL(2)$ representations by identifying almost-flat equivariant representations that are related by the action

$$(\mathcal{X}_1, \mathcal{X}_2, \mathcal{X}_a, \mathcal{X}_4, \mathcal{X}_5) \mapsto (\epsilon_1 \mathcal{X}_1, \epsilon_2 \mathcal{X}_2, \epsilon_a \mathcal{X}_a, \epsilon_4 \mathcal{X}_4, \epsilon_5 \mathcal{X}_5), \quad (6.46)$$

where all the $\epsilon_i = \pm 1$ with the constraints that $\epsilon_1 \epsilon_2 \epsilon_A = 1$ as well as $\epsilon_A \epsilon_4 \epsilon_5 = 1$ [24].¹⁴

6.2.4 Genus two surface

The last Fenchel-Nielsen example that we discuss is the genus two surface. Our goal is to show that the six Fenchel-Nielsen length and twist coordinates occur as spectral coordinates. We choose an (arbitrary) Fenchel-Nielsen network and fix the auxiliary data as in Figure 41.

Let us first verify that there is indeed a six-parameter family of almost-flat equivariant abelian representations ρ^{ab} . There are 15 short paths \wp and 3 nontrivial flatness conditions. Furthermore, there are 6 gauge redundancies (one for each marked point). This leaves us with 6 gauge-invariant abelian holonomies. These can be associated to holonomies along a subset of six 1-cycles $A_{1,2,3}$ and $B_{1,2,3}$, on the cover of the genus two surface, with $A_i \# B_j = \delta_{ij}$.¹⁵

To be explicit, these 1-cycles are lifts of 1-cycles $\alpha_{1,2,3}$ and $\beta_{1,2,3}$ on the genus two surface, which we choose analogous to the four-holed sphere example. That is, we identify each tube in the pants decomposition of the genus two surface with the internal tube of the four-holed sphere, and then choose the two 1-cycles α_k and β_k for this tube as in Figure 40. Any gauge-fixed almost-flat equivariant abelian representation can be expressed in terms of the corresponding six abelian holonomies $\mathcal{X}_{A_{1,2,3}}$ and $\mathcal{X}_{B_{1,2,3}}$.

Again, we can solve the \mathcal{S} -matrices uniquely (by imposing the branch point equations as well fixing the eigenvalues of the non-abelian monodromies around the tubes) and find that they have the expected form for a molecule II type network. It is immediate that the complexified Fenchel-Nielsen length coordinates occur as the spectral coordinates \mathcal{X}_{A_1} , \mathcal{X}_{A_2} and \mathcal{X}_{A_3} . To find the Fenchel-Nielsen twist coordinates we compute the $SL(2)$ monodromies around the cycles β_1 , β_2 and β_3 . We find that the spectral coordinates \mathcal{X}_{B_1} , \mathcal{X}_{B_2} and \mathcal{X}_{B_3} are indeed complexified Fenchel-Nielsen twist coordinates, agreeing with the common definition up to a multiplicative term, similar to formula (6.44).

6.3 Mixed networks

Just as for Fenchel-Nielsen and Fock-Goncharov type networks, we can apply the non-abelianization map to any mixed type spectral network. In particular, for the examples

¹⁴Here one has to be careful that the action of the group $(\mathbb{Z}/2\mathbb{Z})^3$ on \mathcal{X}_B is not trivial (since B is not an even cycle). Instead \mathcal{X}_B transforms in the same way as the factor d . The action of $(\mathbb{Z}/2\mathbb{Z})^3$ is trivial on the twist parameter $\tilde{t} = \sqrt{\frac{(\mathcal{X}_a \mathcal{X}_1 - \mathcal{X}_2)(1 - \mathcal{X}_1 \mathcal{X}_2 \mathcal{X}_a)(\mathcal{X}_a \mathcal{X}_5 - \mathcal{X}_4)(1 - \mathcal{X}_a \mathcal{X}_4 \mathcal{X}_5)}{(\mathcal{X}_a \mathcal{X}_2 - \mathcal{X}_1)(\mathcal{X}_1 \mathcal{X}_2 - \mathcal{X}_a)(\mathcal{X}_a \mathcal{X}_4 - \mathcal{X}_5)(\mathcal{X}_4 \mathcal{X}_5 - \mathcal{X}_a)}} t$.

¹⁵There are ten 1-cycles on the genus 5 cover, but the holonomies of an almost-flat equivariant abelian connection around these 1-cycles are not all independent: $\mathcal{X}(\sigma^* \gamma) = \mathcal{X}(\gamma)^{-1}$.

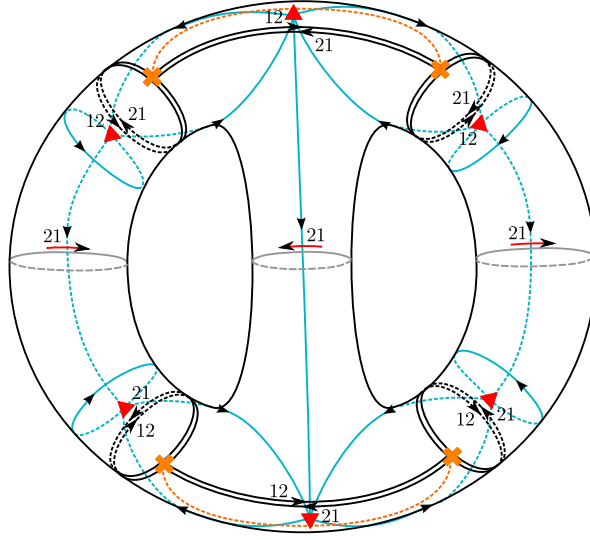


Figure 41: Example of a Fenchel-Nielsen network on the genus two surface, together with a choice of auxiliary data: branch-cut (orange dashed lines), marked points (red triangles), short paths (light blue lines) and a + direction for the pants curves.

discussed in section 2 we find unique solutions for the \mathcal{S} -matrices, that have the same form as described above. I.e. each wall in the resolution of the network contributes with a factor that computes the abelian holonomy of an auxiliary path on Σ . This path starts at a lift of the basepoint along the wall, follows the wall backwards to the nearest branch point, circles around the branch point, and follows the wall in the forward direction to the other lift of the basepoint.

Using this explicit form of the \mathcal{S} -matrices, we obtain the $SL(2)$ flat connection in terms of purely abelian data. We can compute a basis of monodromy matrices in terms of the spectral coordinates, and compare to known coordinate systems. We have done this, and found that not all spectral coordinates for mixed spectral networks can be expressed as Fenchel-Nielsen or Fock-Goncharov coordinates. We leave the further exploration of these coordinates for future work.

7 Some consequences

7.1 Asymptotics

One of the most interesting properties of the spectral coordinates [1] is that they have simple asymptotics when evaluated along certain natural one-parameter families of $SL(2, \mathbb{C})$ -connections. This asymptotic property was described in [3] in the case of Fock-Goncharov spectral networks. One consequence of the constructions described in this paper is that a similar asymptotic property holds for Fenchel-Nielsen coordinates. In this section we briefly describe that story.

We will consider one-parameter families of flat $SL(2, \mathbb{C})$ -connections, $\{\nabla(\zeta)\}_{\zeta \in \mathbb{C}^\times}$. We will not consider arbitrary families, but rather only the ones which come from solutions

of Hitchin equations: given a solution (D, φ) of Hitchin's equations the corresponding family is

$$\nabla(\zeta) = \zeta^{-1}\varphi + D + \zeta\bar{\varphi}. \quad (7.1)$$

Indeed Hitchin's equations for the pair (D, φ) say precisely that the connection $\nabla(\zeta)$ is flat for every $\zeta \in \mathbb{C}^\times$.

Now we ask: how does $\nabla(\zeta)$ behave asymptotically as $\zeta \rightarrow 0$? The answer to this question is somewhat intricate; in particular, it turns out to depend on precisely how ζ approaches 0. One can get simpler answers if one restricts ζ to lie in a half-plane, say the open half-plane \mathcal{H}_θ centered on the ray $e^{i\theta}\mathbb{R}_+$, and if one chooses the correct coordinate system on the moduli of flat connections. Namely, given the Higgs field φ , we consider the quadratic differential

$$\varphi_2 = \text{Tr}(e^{2i\theta}\varphi^2). \quad (7.2)$$

As described in § 3, this quadratic differential corresponds to a particular spectral curve $\Sigma \subset T^*C$ and spectral network $\mathcal{W}(\varphi_2)$. This spectral network induces spectral coordinate functions \mathcal{X}_γ . The $\zeta \rightarrow 0$ asymptotics of the spectral coordinates of the family $\nabla(\zeta)$ were studied in [3, 1], where it was argued that they are controlled by the periods of the spectral curve:

$$\mathcal{X}_\gamma(\nabla(\zeta)) \sim c_\gamma \exp\left(\zeta^{-1} \oint_\gamma \lambda\right) \quad (7.3)$$

where c_γ is ζ -independent, and λ denotes the tautological (Liouville) 1-form on T^*C .

In particular, suppose φ is a generic Higgs field, so that φ_2 is a generic quadratic differential. In this case the spectral network $\mathcal{W}(\varphi_2)$ is a Fock-Goncharov network, and the corresponding coordinates are Fock-Goncharov coordinates. Thus (7.3) tells us the asymptotic behavior of the Fock-Goncharov coordinates of the connections $\nabla(\zeta)$. These asymptotics were derived using the WKB approximation in [3], and a more general method of obtaining them was described in [1].

On the other hand, suppose that φ is a special Higgs field, such that φ_2 is a Strebel differential. In this case $\mathcal{W}(\varphi_2)$ is a Fenchel-Nielsen network, and (7.3) tells us the asymptotic behavior of the Fenchel-Nielsen coordinates of $\nabla(\zeta)$. (More precisely, the spectral coordinates associated to $\mathcal{W}(\varphi_2)$ depend on whether we take the British or American resolution; the asymptotics (7.3) in the open half-plane \mathcal{H}_θ apply to either. We believe that for the British resolution the asymptotics extend also to one of the rays on the *boundary* of the half-plane, and for the American resolution they extend to the other boundary. It would be useful to verify this by direct application of the WKB approximation.)

Remember that the periods $\oint_\gamma \lambda$ are real-valued when φ_2 is a Strebel differential and γ is the lift to Σ of a pants curve on C . The Fenchel-Nielsen length coordinates thus behave asymptotically as the exponentials of a set of real period integrals. This makes precise the identification between Coulomb parameters and length coordinates that follows from the AGT correspondence.

7.2 Line defects

A second interesting consequence of our discussion concerns the physics of line defects.

Recall from [26, 27] that, in the theory $S[A_1, C]$ associated to a punctured Riemann surface C , there is a class of supersymmetric line defects $L(\wp, \zeta)$ labeled by closed loops \wp on C and phases $\zeta \in \mathbb{C}^\times$.

According to [27], the spectrum of framed BPS states attached to $L(\wp, \zeta)$ can be read off from the abelianization map, as follows. Let M denote the holonomy of an $SL(2, \mathbb{C})$ connection around \wp . Given any spectral network \mathcal{W} , the \mathcal{W} -abelianization map expresses $\text{Tr } M$ as a sum of abelian holonomies

$$\text{Tr } M = \sum_{\gamma} \overline{\Omega}(\wp, \gamma, \mathcal{W}) \mathcal{X}_{\gamma}, \quad (7.4)$$

where the coefficients $\overline{\Omega}(\wp, \gamma, \mathcal{W}) \in \mathbb{Z}$. If \mathcal{W} is the WKB spectral network corresponding to a quadratic differential φ_2/ζ^2 , then these coefficients have a physical interpretation: $\overline{\Omega}(\wp, \gamma, \mathcal{W})$ counts the framed BPS states of charge γ attached to the line defect $L(\wp, \zeta)$, at the point of the Coulomb branch determined by φ_2 .

If φ_2 is generic, and \wp is not a cycle contractible to a puncture, this always leads to at least three framed BPS states. However, if \mathcal{W} happens to be a Fenchel-Nielsen network, or more generally a mixed network whose complement contains at least one annulus A , then we may take \wp to be a path going around A . In this case, \mathcal{W} -abelianization for \wp is very simple: \wp crosses no S -walls at all, so

$$\text{Tr } M = \mathcal{X}_{\gamma} + \mathcal{X}_{-\gamma} \quad (7.5)$$

where γ and $-\gamma$ are the two lifts of \wp to the double cover Σ . Thus, in this situation the supersymmetric line defect $L(\gamma, \zeta)$ supports just two framed BPS states, carrying charges $\gamma, -\gamma$.

Physically we would interpret this in the following way. Let us choose a particular way of looking at the theory $S[A_1, C]$, in which this theory is obtained by gauging a particular $SU(2)$ symmetry in another theory $S[A_1, C']$, with C' obtained from C by cutting along the annulus A . From this point of view, the line defect $L(\wp, \zeta)$ is a Wilson line for the new $SU(2)$ gauge symmetry, in the fundamental representation. Naive classical reasoning would suggest that in the IR this defect should support two framed BPS states, corresponding to the decomposition of the fundamental representation into two weight spaces under $U(1) \subset SU(2)$. At generic (φ_2, ζ) this classical reasoning is not exactly correct: we do get these two states but we get additional states as well. What we have found here is that, if (φ_2, ζ) are chosen specially, the classical picture is precisely correct. (See also some related discussion in [28]).

It would be very interesting to have a direct physical understanding of *why* this simplification occurs.

References

- [1] D. Gaiotto, G. W. Moore, and A. Neitzke, ‘‘Spectral networks,’’ [1204.4824](#).
- [2] D. Gaiotto, ‘‘N=2 dualities,’’ [0904.2715](#).

- [3] D. Gaiotto, G. W. Moore, and A. Neitzke, “Wall-crossing, Hitchin Systems, and the WKB Approximation,” [0907.3987](#).
- [4] D. Gaiotto, G. W. Moore, and A. Neitzke, “Spectral Networks and Snakes,” [1209.0866](#).
- [5] D. Galakhov, P. Longhi, T. Mainiero, G. W. Moore, and A. Neitzke, “Wild Wall Crossing and BPS Giants,” [1305.5454](#).
- [6] K. Hori, C. Y. Park, and Y. Tachikawa, “2d SCFTs from M2-branes,” [1309.3036](#).
- [7] K. Maruyoshi, C. Y. Park, and W. Yan, “BPS spectrum of Argyres-Douglas theory via spectral network,” [1309.3050](#).
- [8] T. Aoki, T. Kawai, S. Sasaki, A. Shudo, and Y. Takei, “Virtual turning points and bifurcation of Stokes curves for higher order ordinary differential equations,” *J. Phys. A* **38** (2005), no. 15, 3317–3336, [math-ph/0409005](#).
- [9] V. Fock and A. Goncharov, “Moduli spaces of local systems and higher Teichmüller theory,” *Publ. Math. Inst. Hautes Études Sci.* (2006), no. 103, 1–211, [math/0311149](#).
- [10] W. Fenchel and J. Nielsen, “Discontinuous groups of isometries in the hyperbolic plane,” *Edited by Asmus L. Schmidt, de Gruyter* (2003).
- [11] S. Wolpert, “The length spectra as moduli for compact Riemann surfaces,” *Annals of Maths* **109** (1979) 323–351.
- [12] S. Wolpert, “The Fenchel-Nielsen deformation,” *Annals of Maths* **115** (1982) 501–528.
- [13] C. Kourouniotis, “Complex length coordinates for quasi-Fuchsian groups,” *Mathematika* **41** (1994) 173–188.
- [14] S. P. Tan, “Complex Fenchel–Nielsen coordinates for quasi-Fuchsian structures,” *Internat. J. Math.* **5** (1994) 239–251.
- [15] N. Nekrasov, A. Rosly, and S. Shatashvili, “Darboux coordinates, Yang-Yang functional, and gauge theory,” [1103.3919](#).
- [16] E. Witten, “Solutions of four-dimensional field theories via M-theory,” *Nucl. Phys.* **B500** (1997) 3–42, [hep-th/9703166](#).
- [17] L. F. Alday, D. Gaiotto, and Y. Tachikawa, “Liouville Correlation Functions from Four-dimensional Gauge Theories,” *Lett. Math. Phys.* **91** (2010) 167–197, [0906.3219](#).
- [18] J. Teschner, “Quantization of the Hitchin moduli spaces, Liouville theory, and the geometric Langlands correspondence I,” *Adv.Theor.Math.Phys.* **15** (2011) 471–564, [1005.2846](#).
- [19] V. Pestun, “Localization of gauge theory on a four-sphere and supersymmetric Wilson loops,” *Commun.Math.Phys.* **313** (2012) 71–129, [0712.2824](#).
- [20] J. Hubbard and H. Masur, “Quadratic differentials and foliations,” *Acta Mathematica* **142** (1979) 221–274.
- [21] V. V. Fock and A. A. Rosly, “Poisson structure on moduli of flat connections on Riemann surfaces and r-matrix,” [math.QA/9802054](#).

- [22] M. F. Atiyah and R. Bott, "The Yang-Mills equations over Riemann surfaces," *Philos. Trans. Roy. Soc. London Ser. A* **308** (1983), no. 1505, 523–615.
- [23] V. Fock, "Dual Teichmüller spaces," [9702018](#).
- [24] Y. Kabaya, "Parametrization of $\mathrm{PSL}(2, \mathbb{C})$ -representations of surface groups," [1110.6674](#).
- [25] T. Okai, "Effects of a change of pants decompositions on their Fenchel–Nielsen coordinates," *Kobe J. Maths.* **10** (1993) 215–223.
- [26] N. Drukker, D. R. Morrison, and T. Okuda, "Loop operators and S-duality from curves on Riemann surfaces," [0907.2593](#).
- [27] D. Gaiotto, G. W. Moore, and A. Neitzke, "Framed BPS States," [1006.0146](#).
- [28] C. Cordova and A. Neitzke, "Line defects, tropicalization, and multi-centered quiver quantum mechanics," [1308.6829](#).